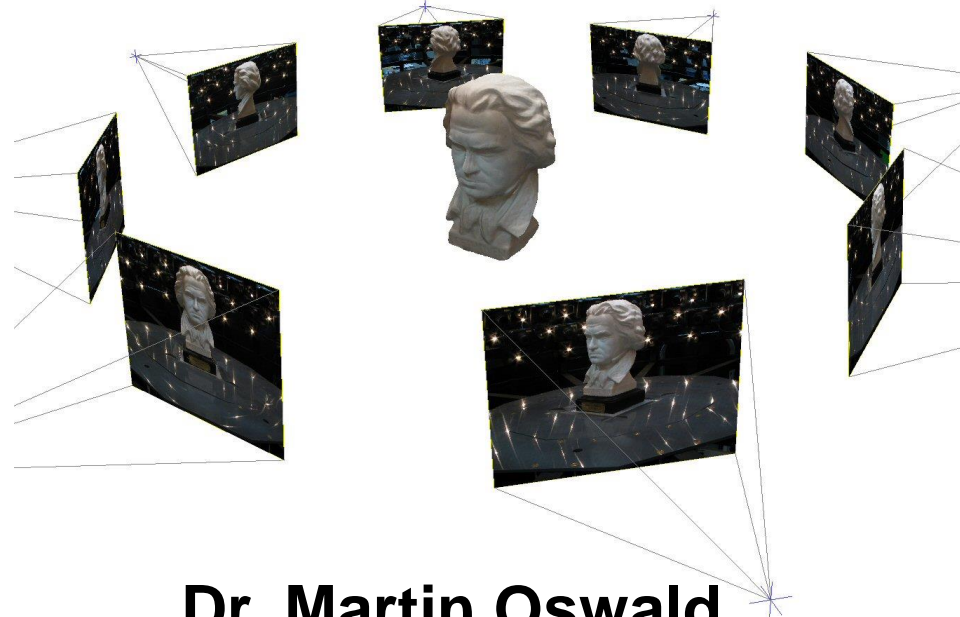


Variational Methods III

Regularizers and Minimal Surface Problems



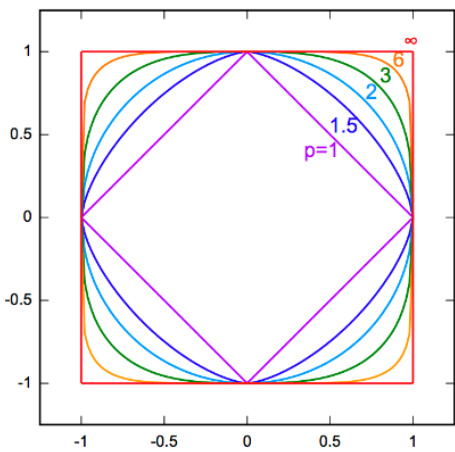
Dr. Martin Oswald

Computer Vision and Geometry Group

Reminder: Norms

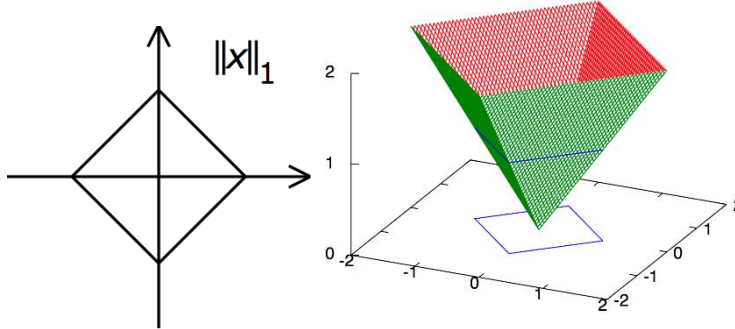
p-norm: $\|x\|_p = \left(\sum_{i=1}^n |x_i|^p \right)^{1/p}$

(convex for $p \geq 1$)



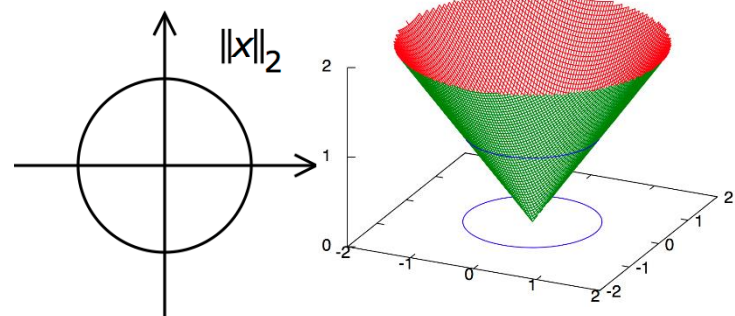
$p = 1$ (Manhattan norm)

$$\|x\|_1 := \sum_{i=1}^n |x_i|$$



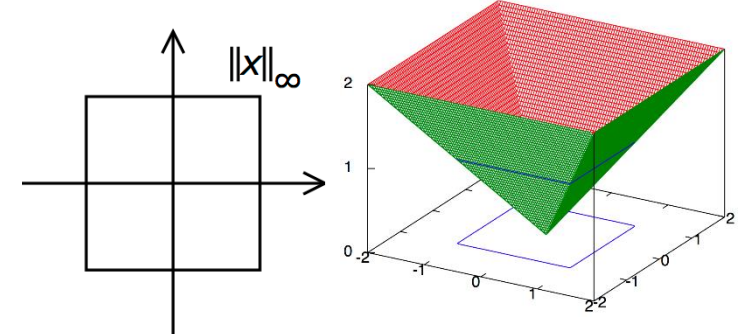
$p = 2$ (Euclidean norm)

$$\|x\|_2 := \sqrt{\sum_{i=1}^n |x_i|^2}$$

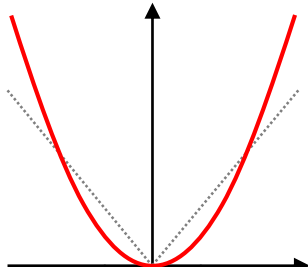
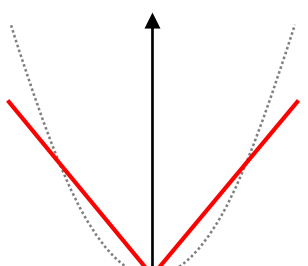
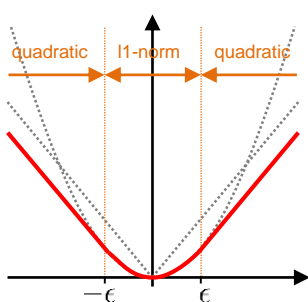


$p = \infty$ (Maximum norm)

$$\|x\|_\infty := \max(|x_1|, \dots, |x_n|)$$



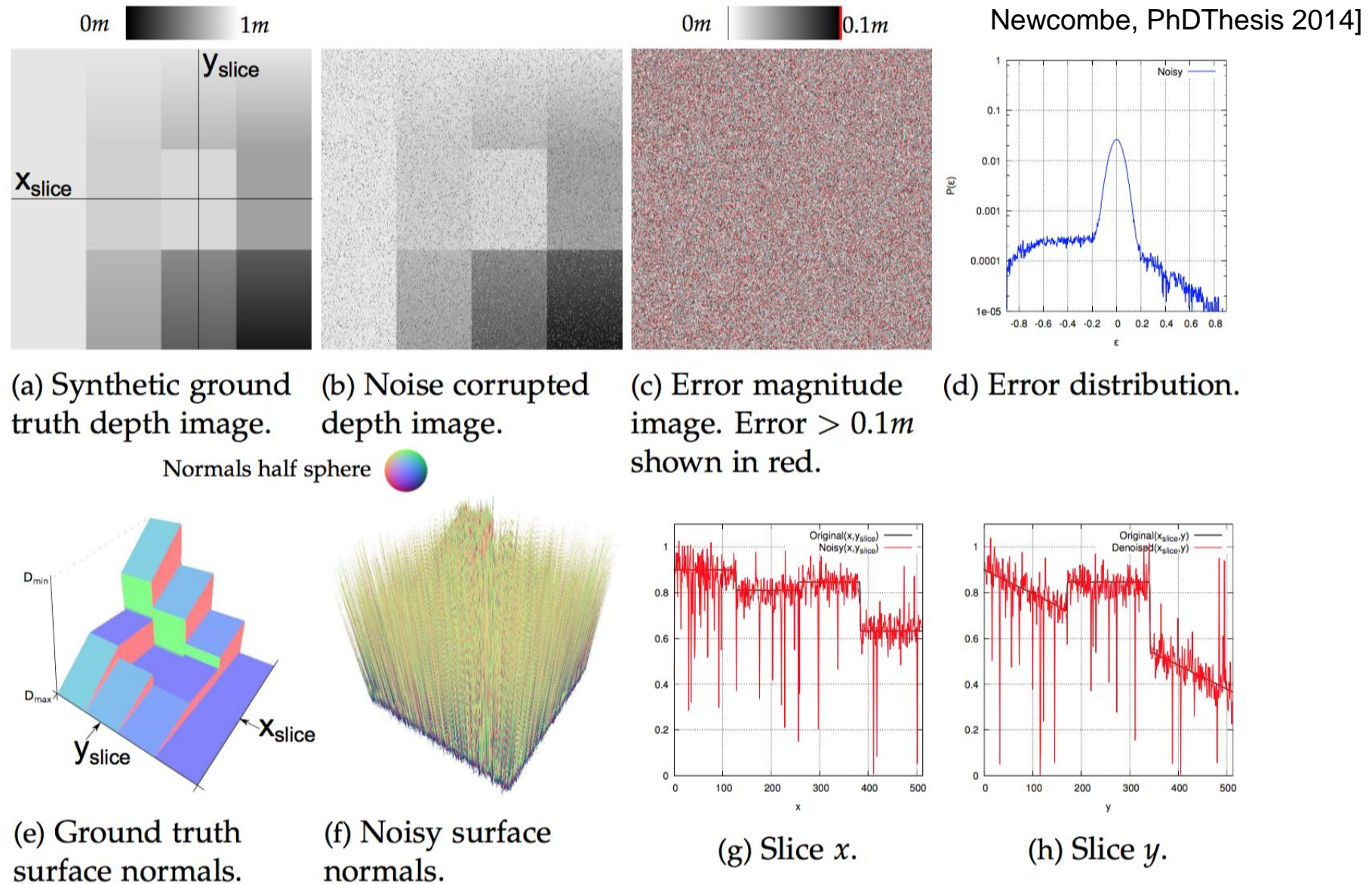
Convex Norms

	Definition	PDF(x)	Graph	Properties
Quadratic	$\ x\ _2^2 := \sum_{i=1}^n x_i ^2$	Gaussian		<ul style="list-style-type: none"> favors smooth solutions over-penalizes outliers and larger function changes differentiable
l_1 -norm	$\ x\ _1 := \sum_{i=1}^n x_i $	Laplacian		<ul style="list-style-type: none"> favors piecewise-constant solutions robust to outliers and preserves larger function changes problem: stair-casing not differentiable at zero
Huber-norm	$\ x\ _\epsilon := \begin{cases} \frac{1}{2\epsilon} x _2^2 & \text{if } x \leq \epsilon \\ x - \frac{\epsilon}{2} & \text{otherwise} \end{cases}$	Hybrid		<ul style="list-style-type: none"> favors piecewise-smooth solutions robust to outliers and preserves larger function changes avoids stair-casing differentiable

Comparison of Convex Norms

Example: depth map denoising
Given: noisy depth map d

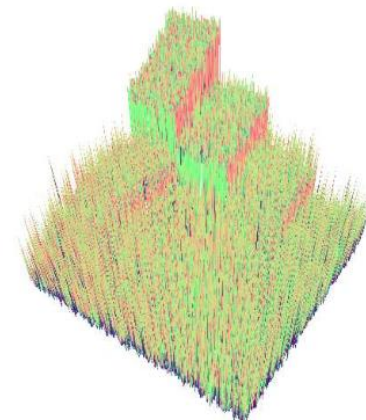
$$E(u) = \lambda \int_{\Omega} \phi_R(\nabla u) dx + \int_{\Omega} \phi_D(u - d) dx$$



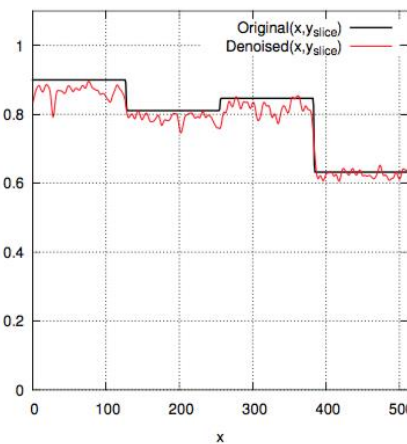
Comparison of Convex Norms

Quadratic-l2 penalization
(Gaussian convolution)

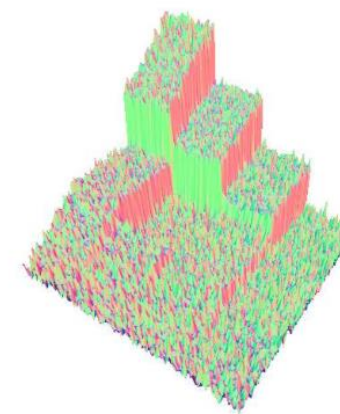
$$E(u) = \lambda \int_{\Omega} \|\nabla u\|_2^2 \, dx \\ + \int_{\Omega} \|u - d\|_2^2 \, dx$$



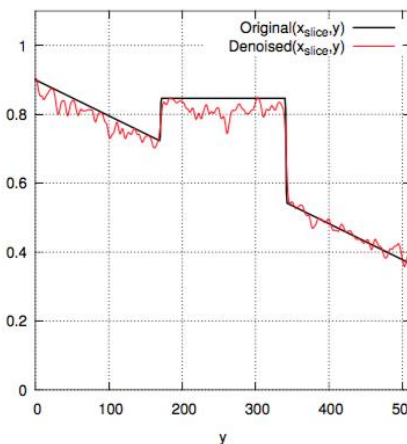
(a) $\sigma = 0.75$



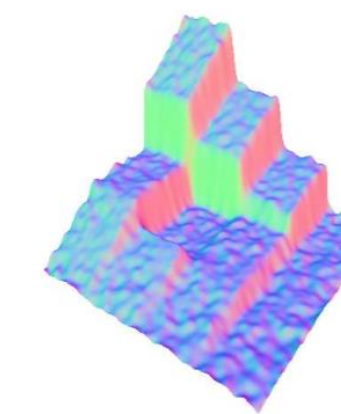
(e) Slice through x ,
 $\sigma = 2.1$



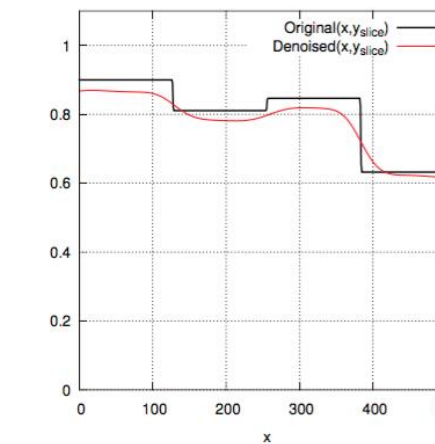
(b) $\sigma = 2.1$



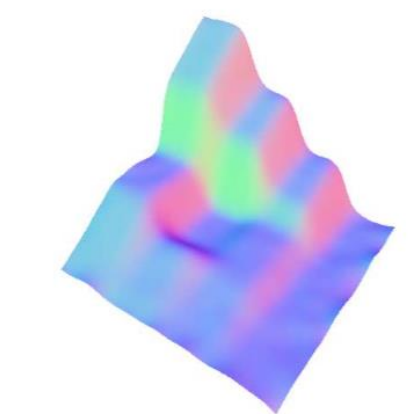
(f) Slice through y ,
 $\sigma = 2.1$



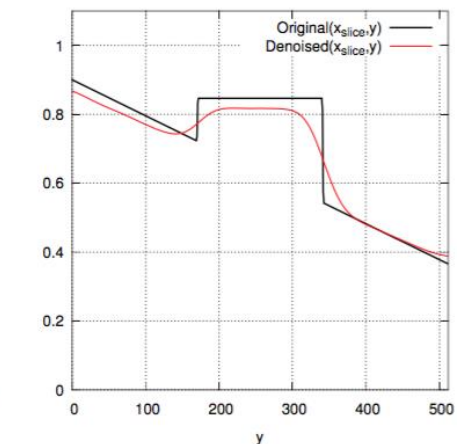
(c) $\sigma = 7.0$



(g) Slice through x ,
 $\sigma = 20$



(d) $\sigma = 20$



(h) Slice through y ,
 $\sigma = 20$

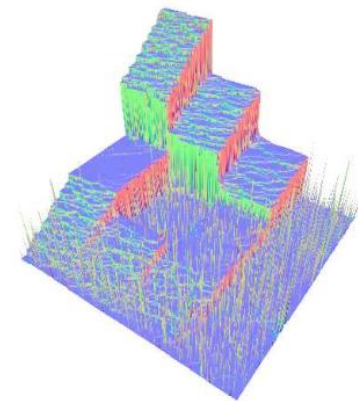
Newcombe, PhDThesis 2014]

Comparison of Convex Norms

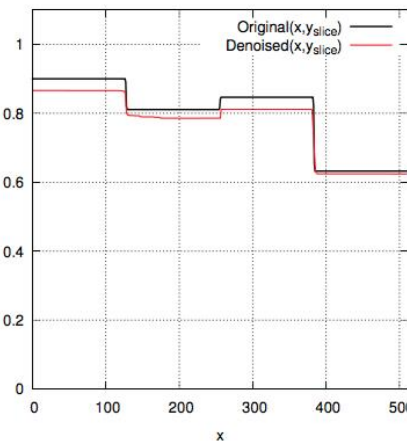
Newcombe, PhD Thesis 2014]

TV-L2 penalization

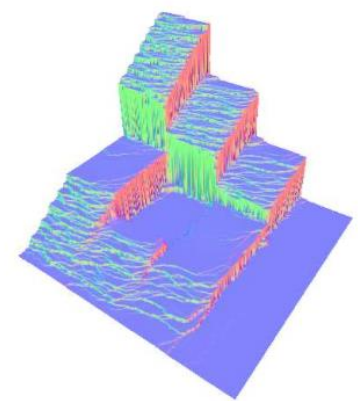
$$E(u) = \lambda \int_{\Omega} \|\nabla u\|_2 \, dx + \int_{\Omega} \|u - d\|_2^2 \, dx$$



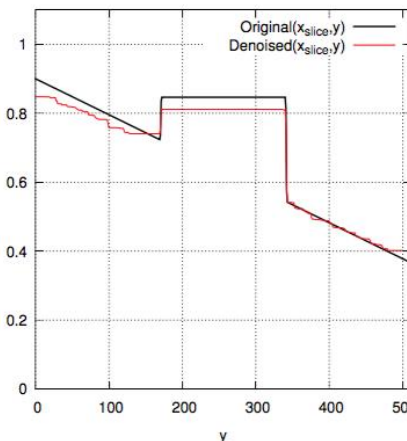
(a) $\lambda = 0.5$



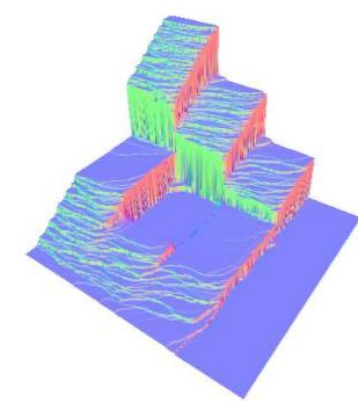
(e) Slice through x ,
 $\lambda = 0.624$



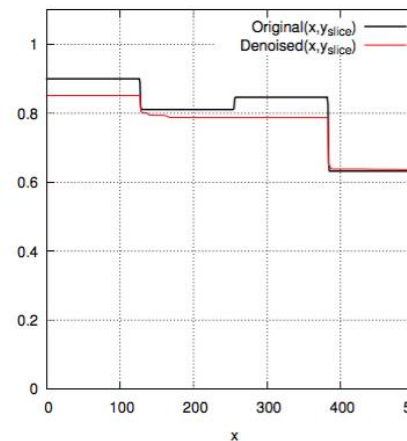
(b) $\lambda = 0.624$



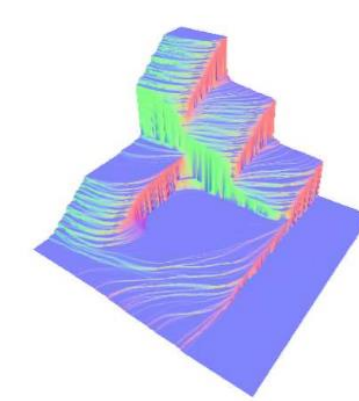
(f) Slice through y ,
 $\lambda = 0.624$



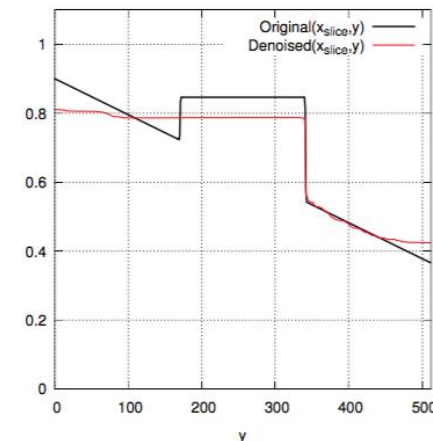
(c) $\lambda = 0.747$



(g) Slice through x ,
 $\lambda = 1.4$



(d) $\lambda = 1.4$



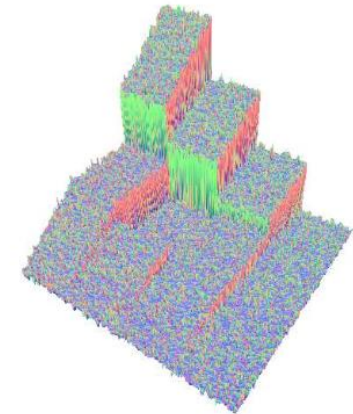
(h) Slice through y ,
 $\lambda = 1.4$

Comparison of Convex Norms

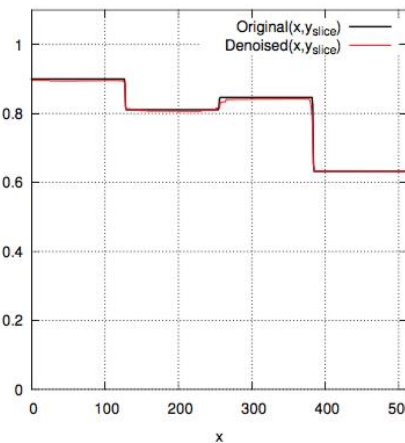
Newcombe. PhD Thesis 2014

TV-L1 penalization

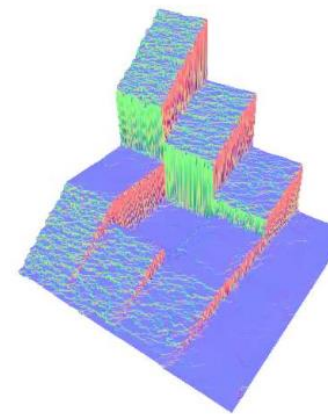
$$E(u) = \lambda \int_{\Omega} \|\nabla u\|_2 \, dx \\ + \int_{\Omega} \|u - d\|_2 \, dx$$



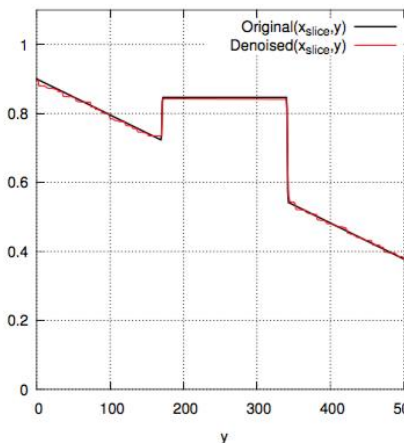
(a) $\lambda = 0.84$



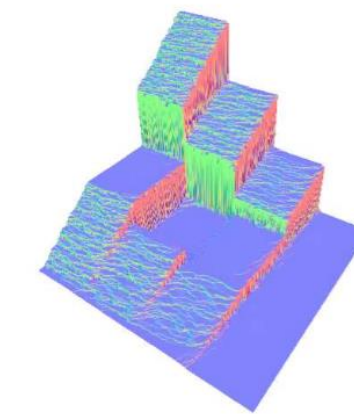
(e) Slice through x ,
 $\lambda = 1.18$



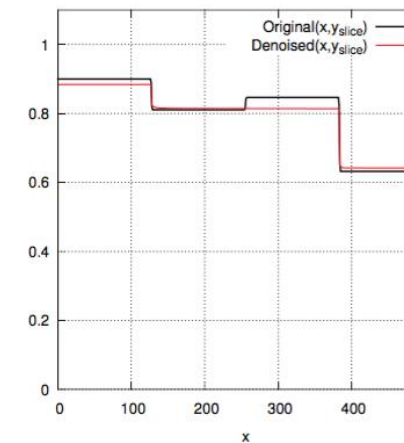
(b) $\lambda = 1.18$



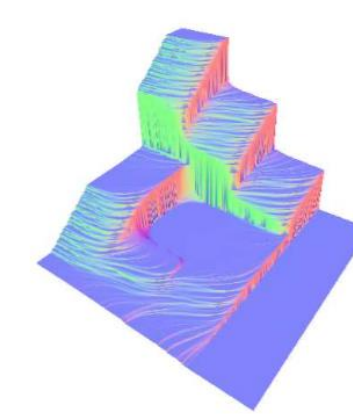
(f) Slice through y ,
 $\lambda = 1.18$



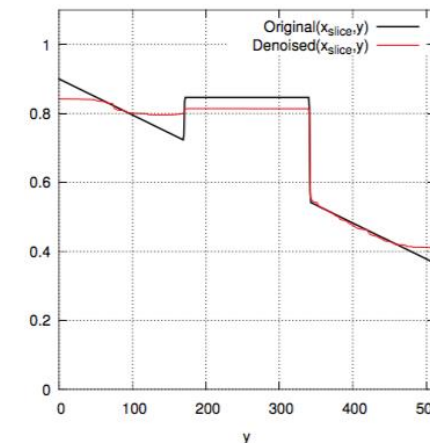
(c) $\lambda = 1.53$



(g) Slice through x ,
 $\lambda = 4.64$



(d) $\lambda = 4.64$



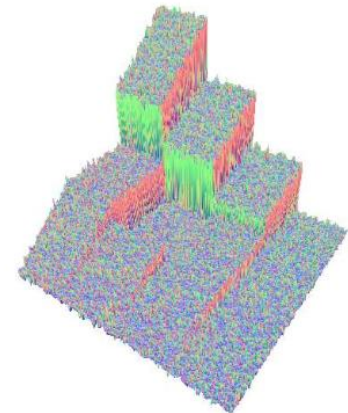
(h) Slice through y ,
 $\lambda = 4.64$

Comparison of Convex Norms

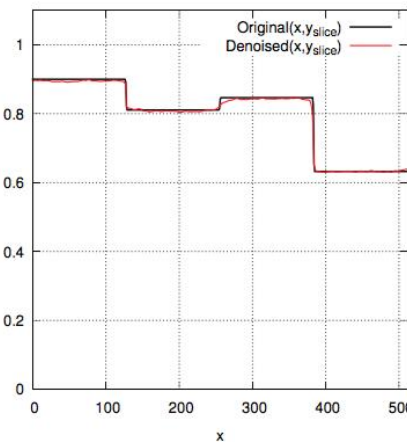
Newcombe, PhD Thesis 2014]

Huber-TV-L1 penalization

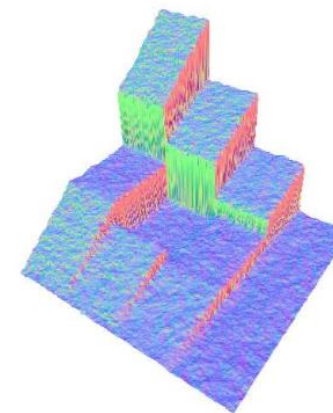
$$E(u) = \lambda \int_{\Omega} \|\nabla u\|_{\epsilon} dx + \int_{\Omega} \|u - d\|_2 dx$$



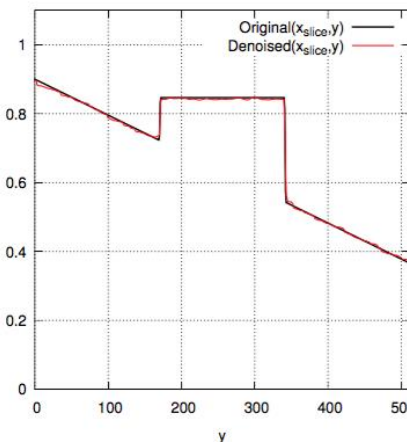
(a) $\lambda = 0.84$



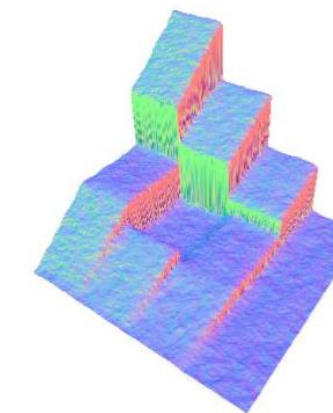
(e) Slice through x ,
 $\lambda = 1.18$



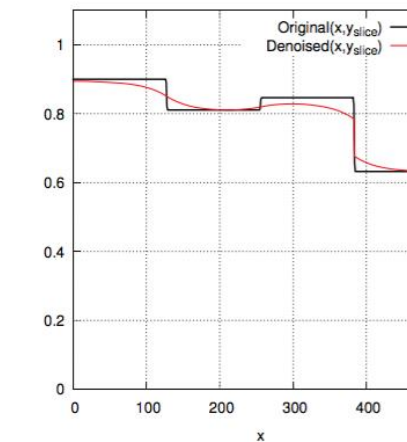
(b) $\lambda = 1.18$



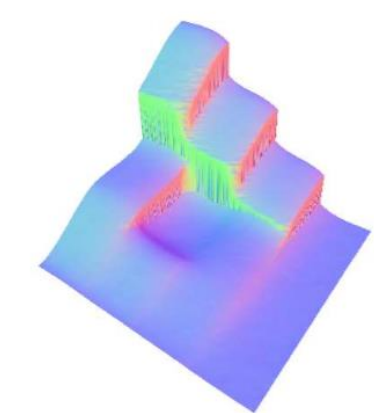
(f) Slice through y ,
 $\lambda = 1.18$



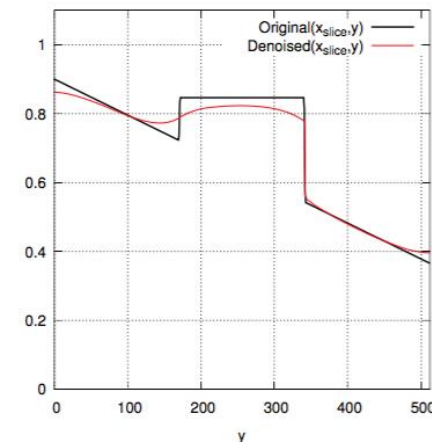
(c) $\lambda = 1.53$



(g) Slice through x ,
 $\lambda = 4.64$



(d) $\lambda = 4.64$

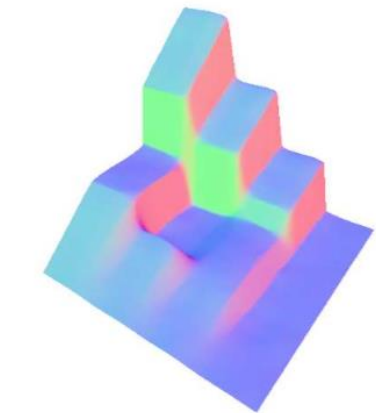
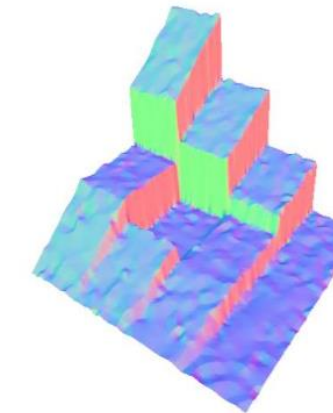
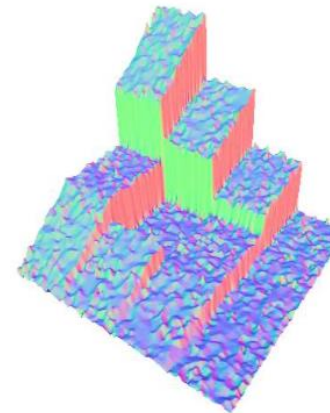
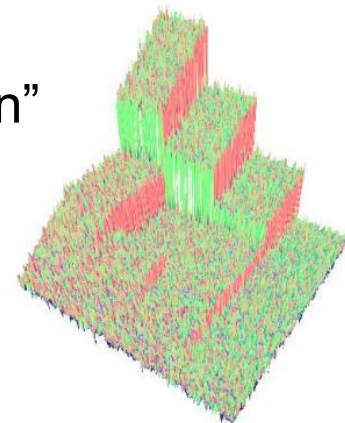


(h) Slice through y ,
 $\lambda = 4.64$

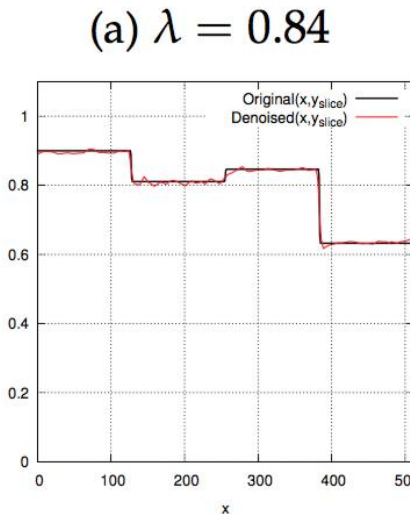
Comparison of Convex Norms

TGV²-I1 penalization
“Total Generalized Variation”
(favors piece-wise affine
solutions)

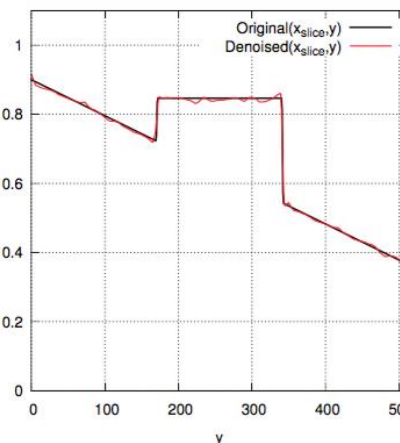
$$E(u) = \alpha_1 \int_{\Omega} \|\nabla u - v\| \, dx \\ + \alpha_0 \int_{\Omega} \|\mathcal{E}(v)\| \, dx \\ + \int_{\Omega} \|u - d\| \, dx$$



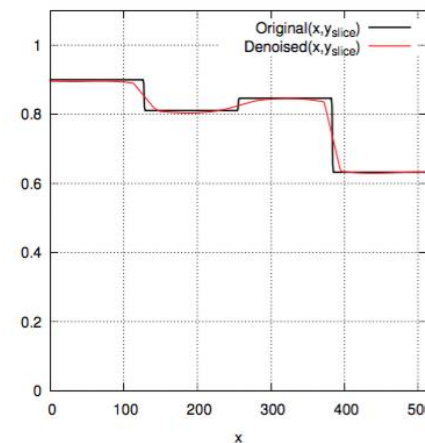
Newcombe, PhD Thesis 2014]



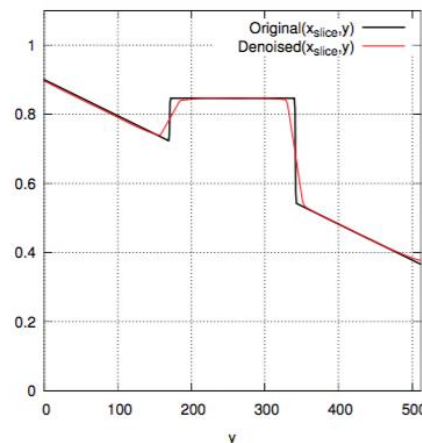
(e) Slice through x ,
 $\lambda = 1.41$



(f) Slice through y ,
 $\lambda = 1.41$



(g) Slice through x ,
 $\lambda = 7.56$



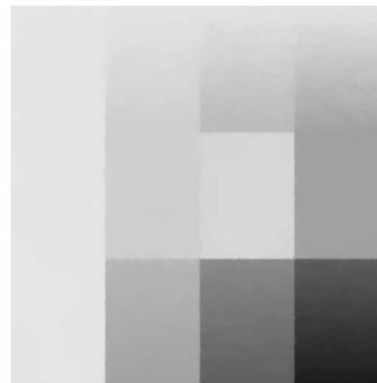
(h) Slice through y ,
 $\lambda = 7.56$

Comparison of Convex Norms

Newcombe, PhD Thesis 2014]

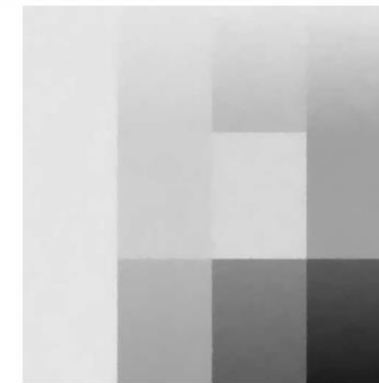
Denoising results

(a) $\text{TV} - \ell_1$,
 $\lambda = 1.18$

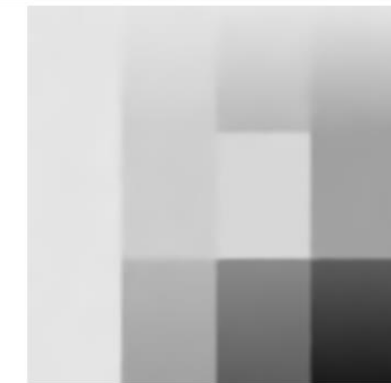


Depth solutions

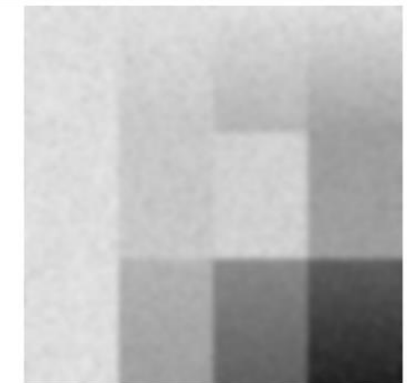
(b) Huber- ℓ_1 ,
 $\lambda = 1.18$,
 $\gamma = 0.00147$



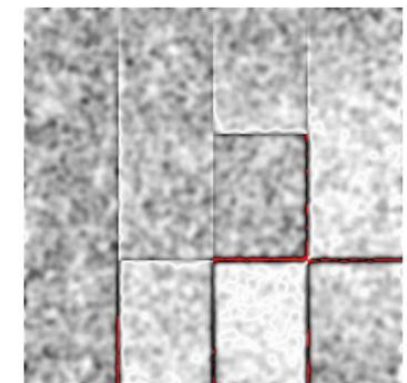
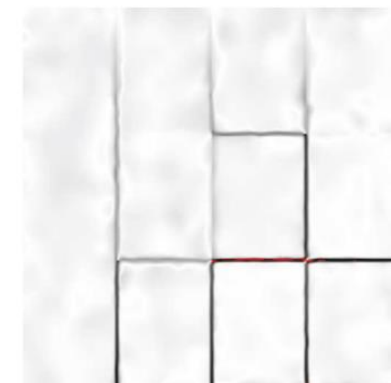
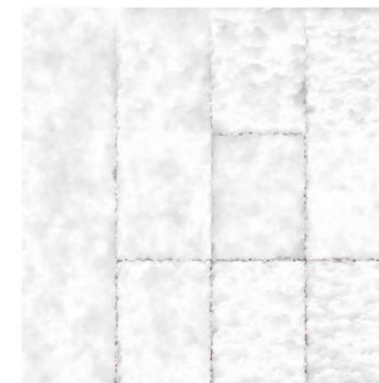
(c) $\text{TGV}_\alpha^2 - \ell_1$,
 $\lambda = 2.53$



(d) Gaussian *,
 $\sigma = 4$



Absolute Error



Graph-cuts vs. Variational Methods

Graph-cuts

- + easy to use, very efficient specialized solvers available (sub-modularity!)
- + faster optimization on a single core
- + non-metric smoothness terms (e.g. triangle inequality does not hold)
- metrification errors
- slow on multiple cores (hard to parallelize)

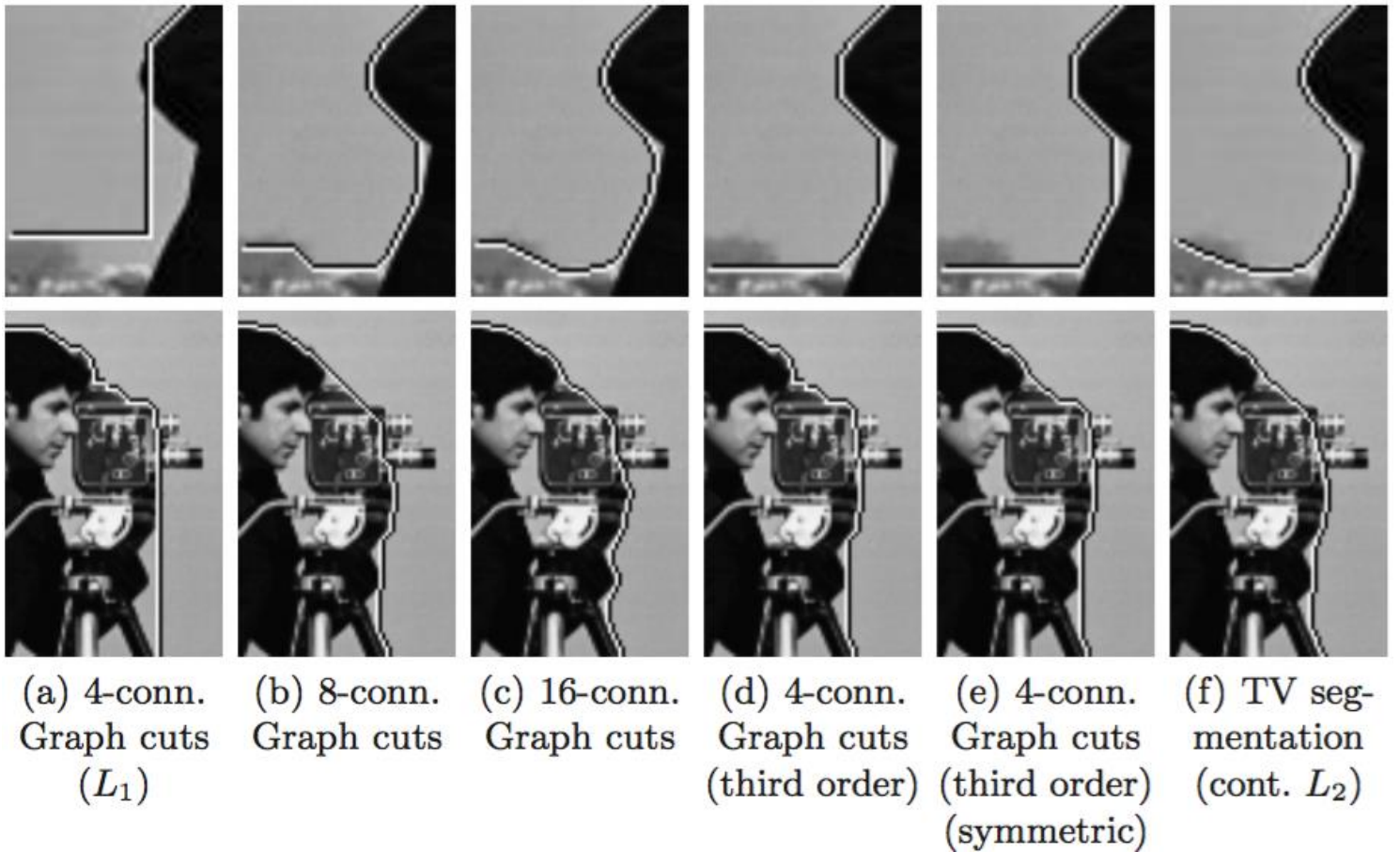
Variational Methods

- + effectively (almost) a generalization of purely discrete methods
- + fast optimization on multiple cores (usually easy to parallelize)
- + sometimes tighter relaxations possible, e.g. multi-label segmentation
- + clean mathematical formulation independent of underlying discretization
effectively a separation of mathematical model and discretization
- slow on single core
- no non-metric smoothness (but continuously inspired approaches possible)

Graph-cuts vs. Variational Methods

Metrication errors of graph-cuts
in image segmentation

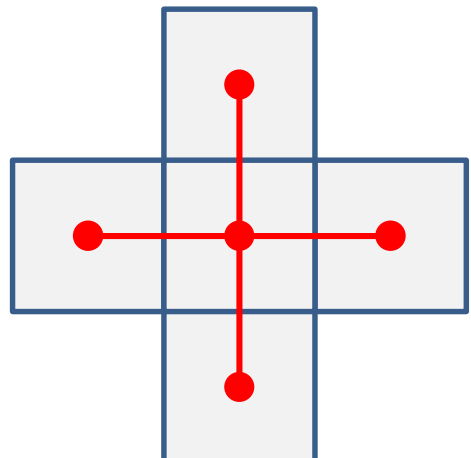
[Klodt et al., ECCV 2008]



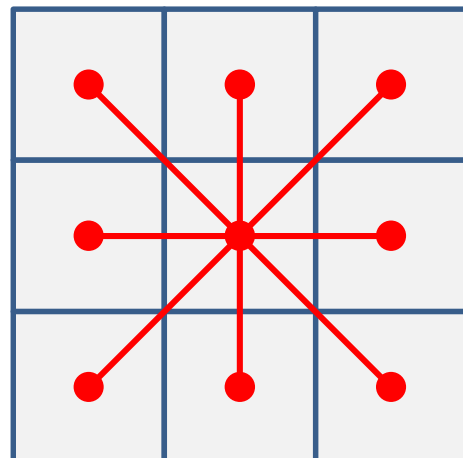
Graph-cuts vs. Variational Methods

Metrication errors of graph-cuts in image segmentation

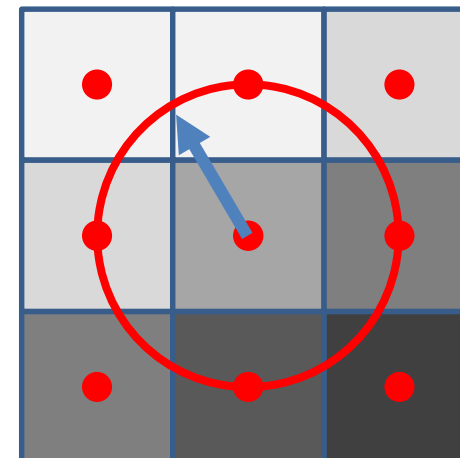
Labels are binary and the Euclidean metric for boundary length penalization can only be approximated with the chosen grid neighborhood structure.



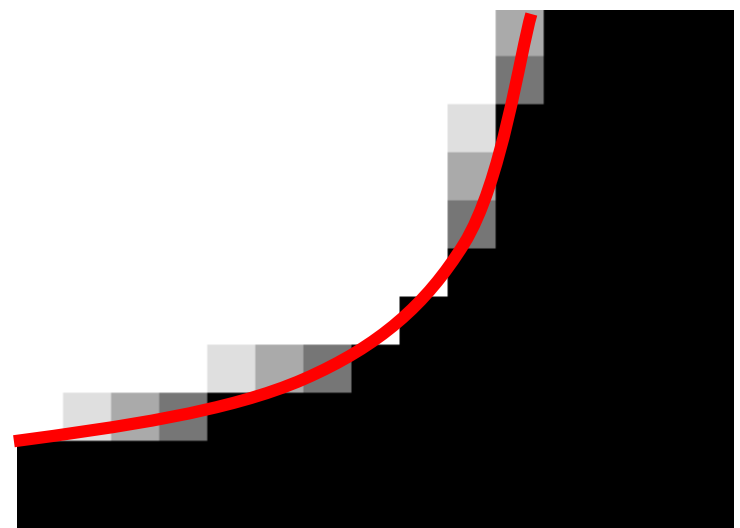
4-neighborhood
(prefers 90 deg.
Solutions)



8-neighborhood
(prefers 45 deg.
Solutions)

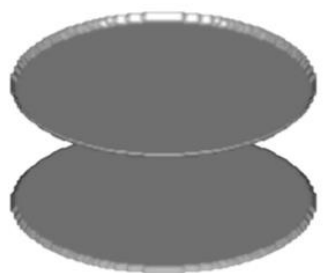


Continuous setting
(any angle with corresponding
penalization possible)

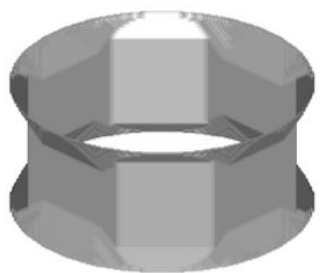


Graph-cuts vs. Variational Methods

Metrication errors of graph-cuts
in surface reconstruction



6-connected
Graph cuts (L_1)



26-connected
Graph cuts

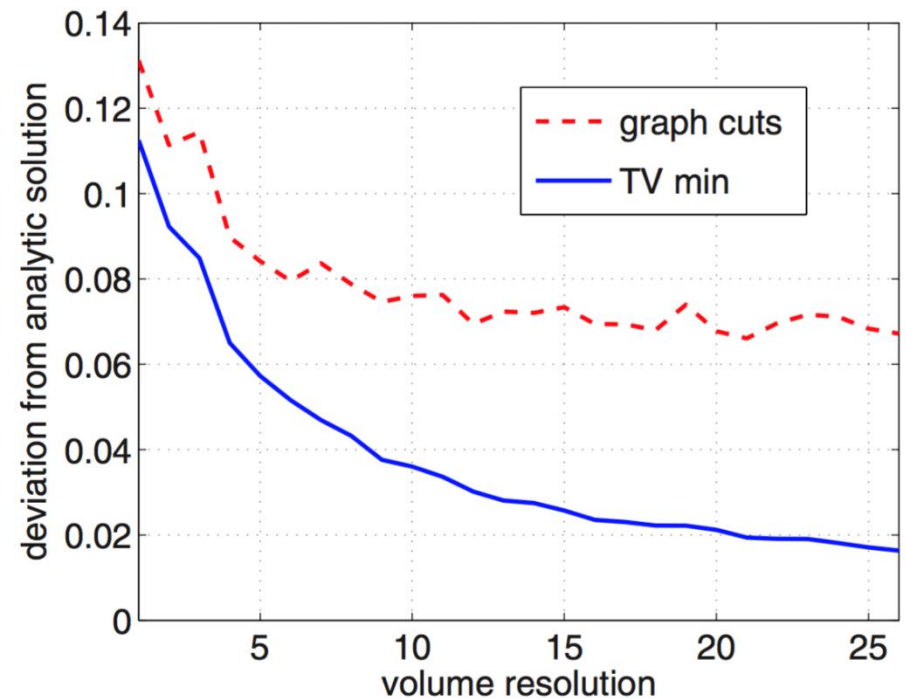


Convex TV
(L_2)



Analytic
Solution

[Klodt et al., ECCV 2008]



Graph-cuts vs. Variational Methods

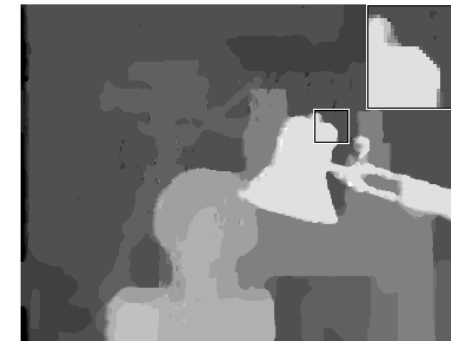
[Pock et al., ECCV 2008]

Stereo reconstruction example: graph-cuts vs. variational approach with functional lifting

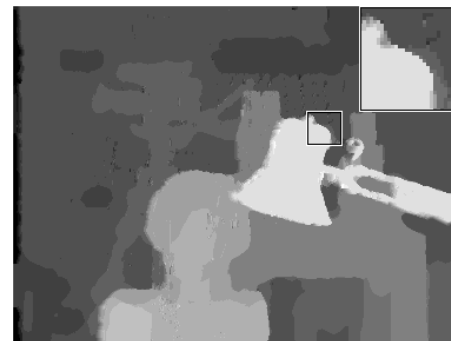
Ishikawa
4-neighborhood



Ishikawa
16-neighborhood



Ishikawa
16-neighborhood



Continuous
formulation



Processing time comparison (GPU: GTX280)

Algorithm	error (%)	Runtime CPU/GPU (sec)	Memory (MB)
Ishikawa 4-neighborhood	2.90	2.9 / -	450
Ishikawa 8-neighborhood	2.63	4.9 / -	630
Ishikawa 16-neighborhood	2.71	14.9 / -	1500
Continuous formulation	2.57	25 / 0.75	54

Equivalence Example: Image Denoising

Image degradation: $f = Hu + \eta$ Noise model: $\eta = \mathcal{G}(0, \sigma)$

MAP-estimate: $u^* = \arg \max_u P(u|f)$ with $P(u|f) = \frac{P(f|u)P(u)}{P(f)}$

prior: $P(u) = \frac{1}{Z} \exp(-\phi(Tu))$ likelihood: $P(f|u) = \prod_{p=1}^N \frac{1}{\sqrt{2\pi}\sigma} \exp\left(-\frac{((Hu)_p - f_p)^2}{2\sigma^2}\right) = \frac{1}{C} \exp\left(-\frac{\|Hu - f\|_2^2}{2\sigma^2}\right)$

$$P(u|f) \propto \exp\left(-\left(\phi(Tu) + \frac{\|Hu - f\|_2^2}{2\sigma^2}\right)\right)$$

$$E(u) = -\log(P(u|f)) = \phi(Tu) + \frac{\|Hu - f\|_2^2}{2\sigma^2}$$

-> Solvable with Graph-cuts or variational approach

The solution of variational approach is equivalent to the graph-cut solution, if the right norm is chosen corresponding to the neighborhood structure in graph-cuts (e.g. Manhattan norm \leftrightarrow 4-neighborhood).

Minimal Surfaces

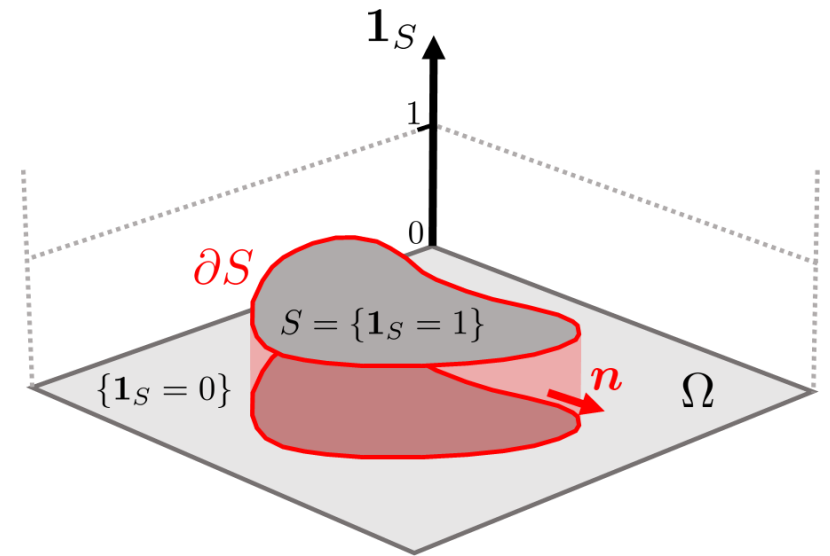
Geometric Properties of the Total Variation

Indicator function

$$\mathbf{1}_S(x) := \begin{cases} 1 & \text{if } x \in S \\ 0 & \text{if } x \notin S \end{cases}$$

Perimeter

$$\text{Per}(S, \Omega) = \text{TV}(\mathbf{1}_S, \Omega)$$



$$\begin{aligned} \text{TV}(\mathbf{1}_S, \Omega) &= \sup_{\|\mathbf{p}\|_\infty \leq 1} \left\{ - \int_{\Omega} \mathbf{1}_S \cdot \text{div}(\mathbf{p}) \, d\mathbf{x} \right\} \\ &= \sup_{\|\mathbf{p}\|_\infty \leq 1} \left\{ - \int_S \text{div}(\mathbf{p}) \, d\mathbf{x} \right\} = \sup_{\|\mathbf{p}\|_\infty \leq 1} \int_{\partial S} \mathbf{n} \cdot \mathbf{p} \, ds = \int_{\partial S} ds = \text{Per}(S, \Omega) \end{aligned}$$

divergence theorem

Minimal Surfaces

Definition (Minimal Surface)

[Meeks and Pérez, 2012]

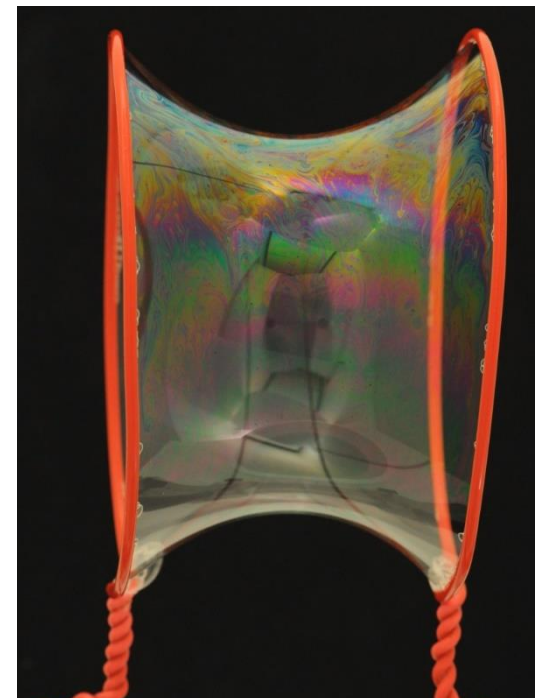
A surface $\Sigma \subset \mathbb{R}^n$ is minimal if and only if it is a critical point of the area functional for all compactly supported variations.

Let $V \subset \mathbb{R}^n$ (e.g. $n=3$) be a domain, $\mathcal{M}(V)$ be the space of $(n-1)$ -dimensional manifolds in V , and $\text{int}(\Sigma)$ be the interior of surface Σ . Further, let $f : V \rightarrow \mathbb{R}$ define the surface shape and $\lambda \in \mathbb{R}_{\geq 0}$ control its smoothness. Then a minimal surface is a minimizer of

$$\Sigma^* \in \arg \min_{\mathcal{M}(V)} \left\{ \text{Per}(\Sigma, V) + \lambda \int_{\text{int}(\Sigma)} f \, dx \right\}$$

Using the properties of the TV for an indicator function $u : V \subset \mathbb{R}^3 \rightarrow \{0, 1\}$ with $u(x) = \mathbf{1}_{\text{int}(\Sigma)}(x)$, this can be equivalently formulated as

$$u^* \in \arg \min_u \left\{ \text{TV}(u, V) + \lambda \int_V f \cdot u \, dx \right\}$$



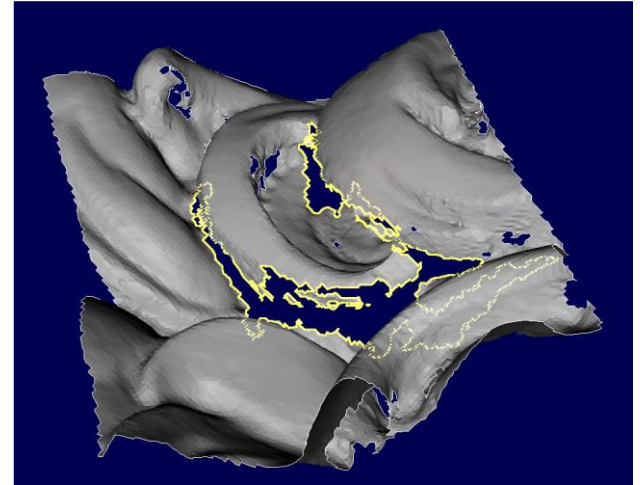
Surface Inpainting

- Surface is represented by an indicator function in the volume.
- Davis et al. performed an explicit diffusion of the indicator function to close holes in the surface
- As we have seen before this can also be solved (more efficiently) by minimizing an appropriate energy, e.g.:

$$E(u) = \int_{\Omega} (|\nabla u|_2^2 + \lambda f u) dx$$



image of Michelangelo's David

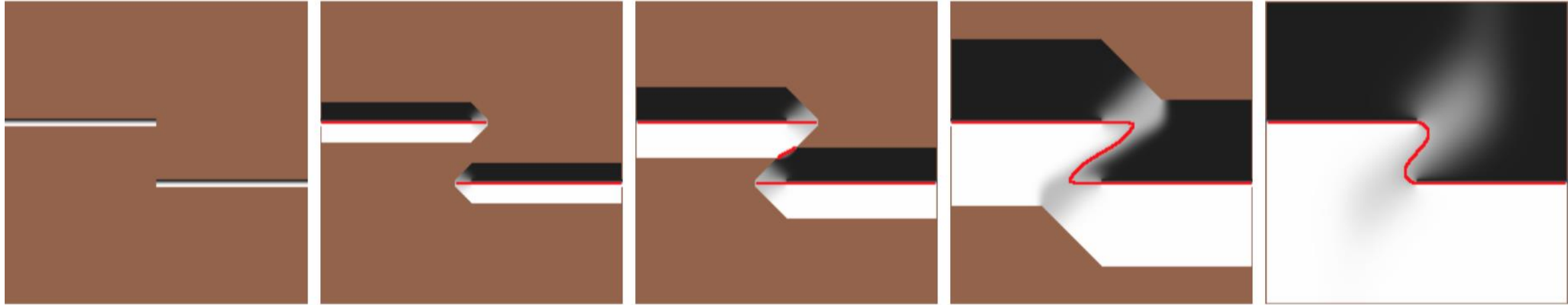


section of a laser scan

- For better results they further integrated line-of-sight constraints (wrt. the sensor position)

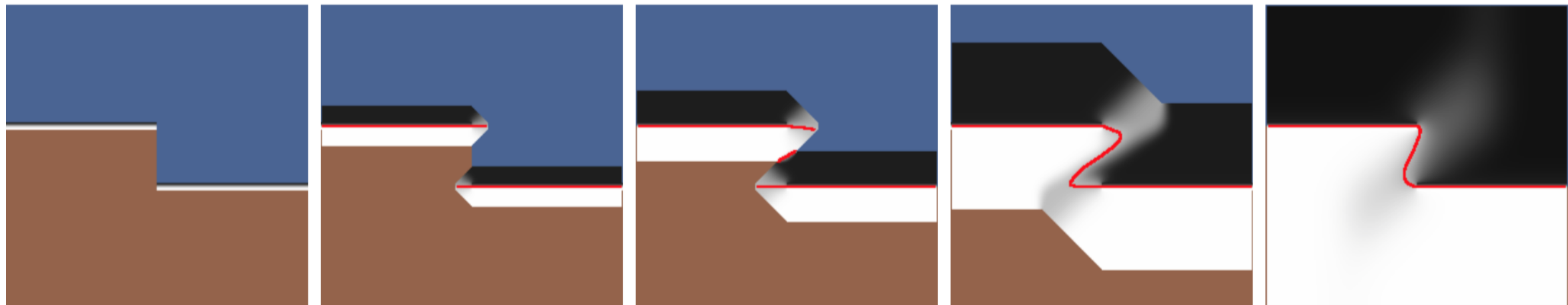
Surface Inpainting

Diffusion process over time



[Davis et al., 3DPVT 2002]

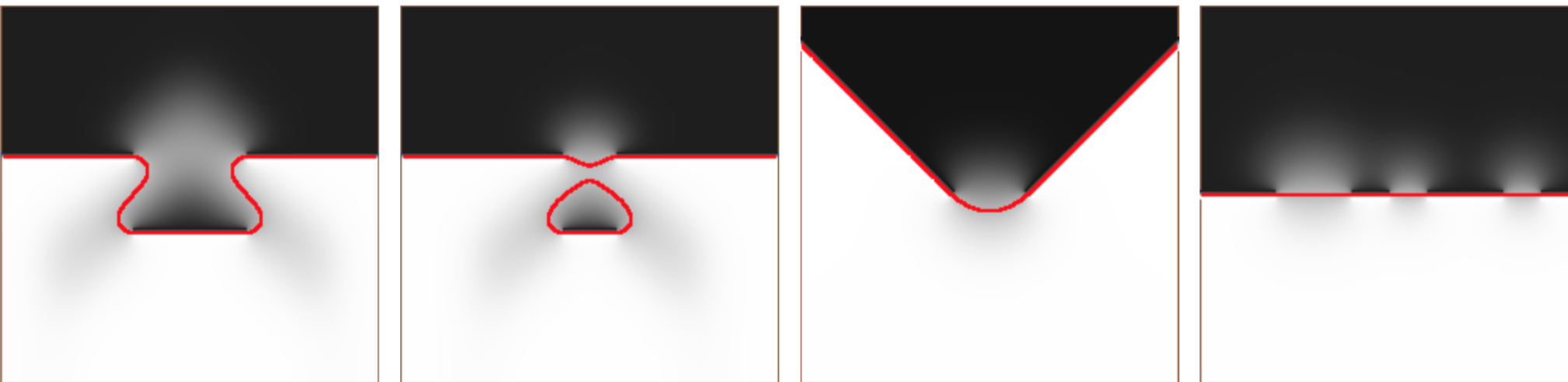
with line of sight constraints



Surface Inpainting

[Davis et al., 3DPVT 2002]

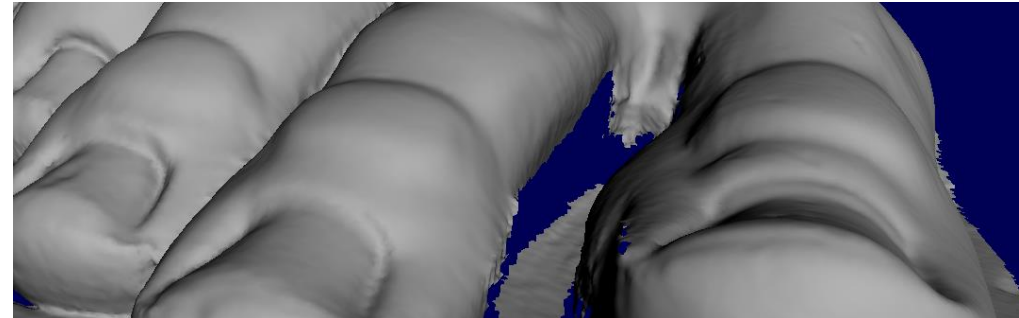
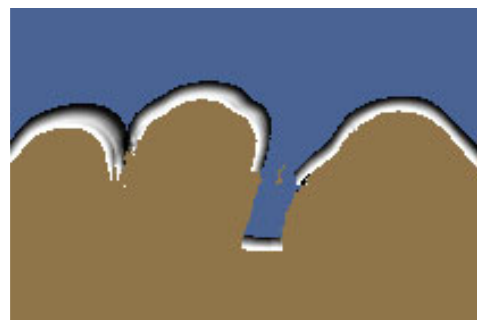
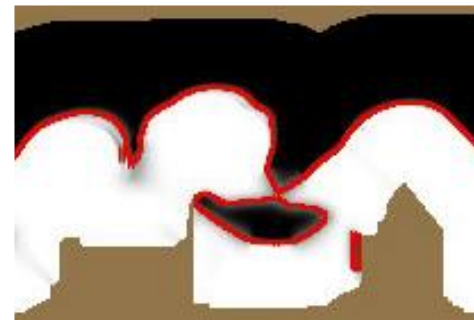
Different types of holes



Surface Inpainting

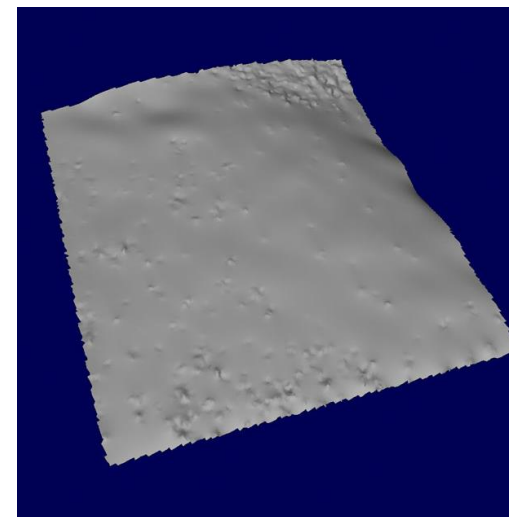
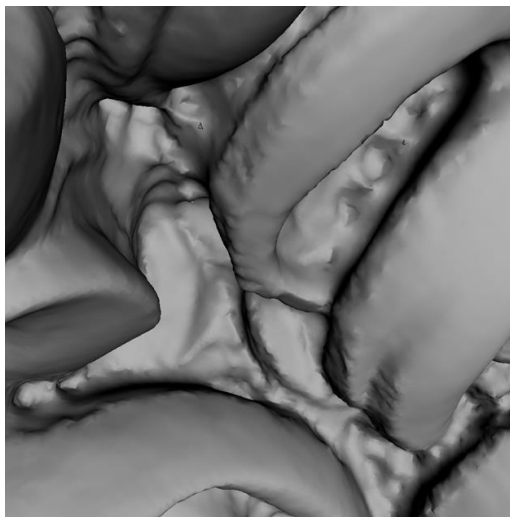
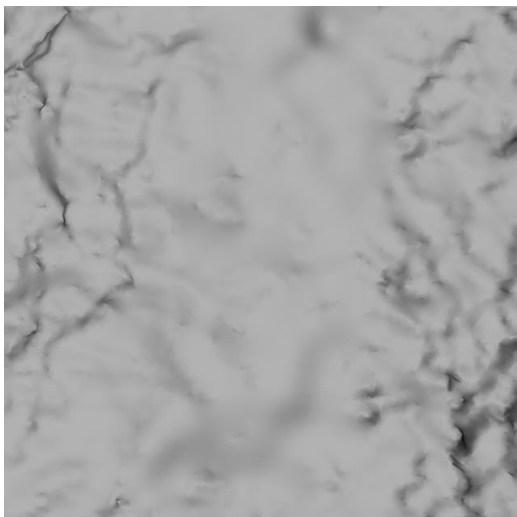
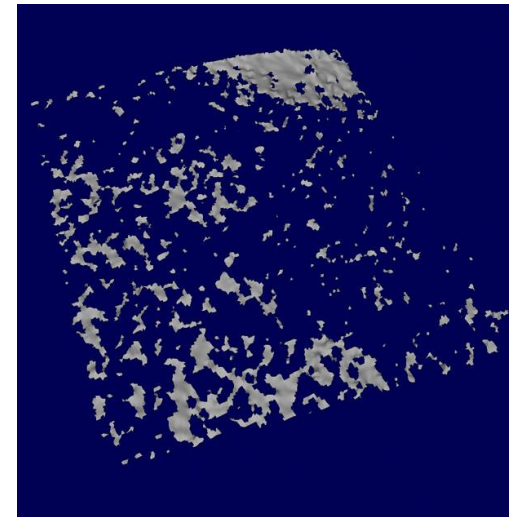
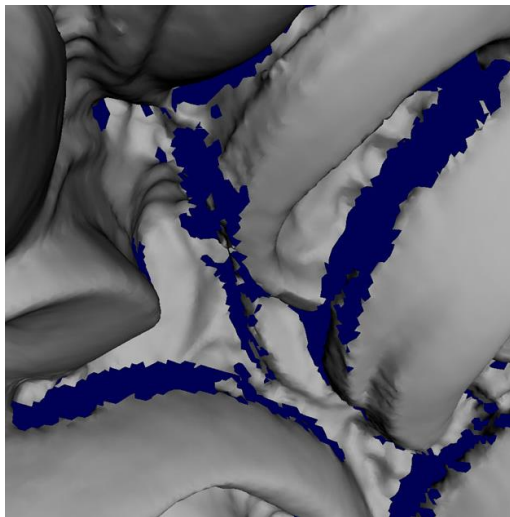
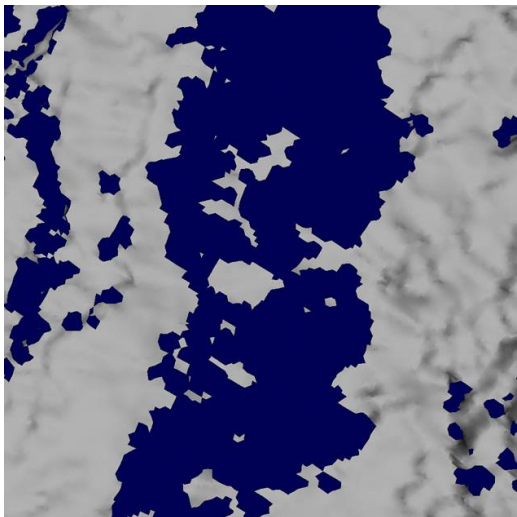
[Davis et al., 3DPVT 2002]

Line of sight constraints



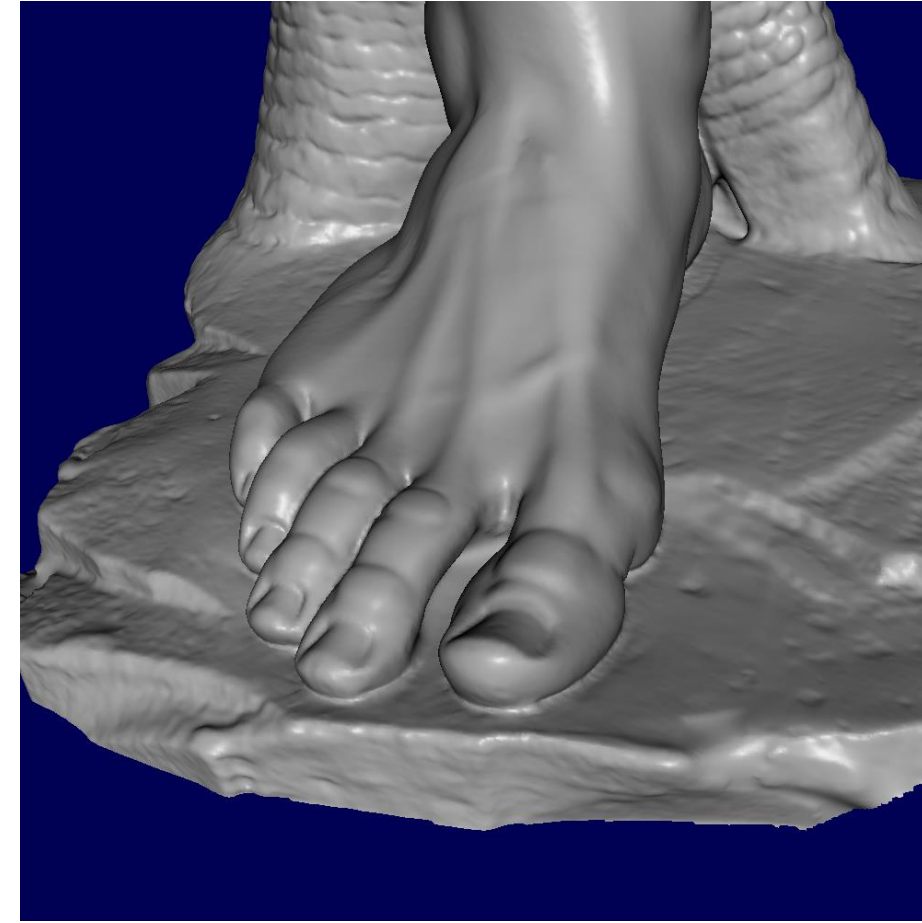
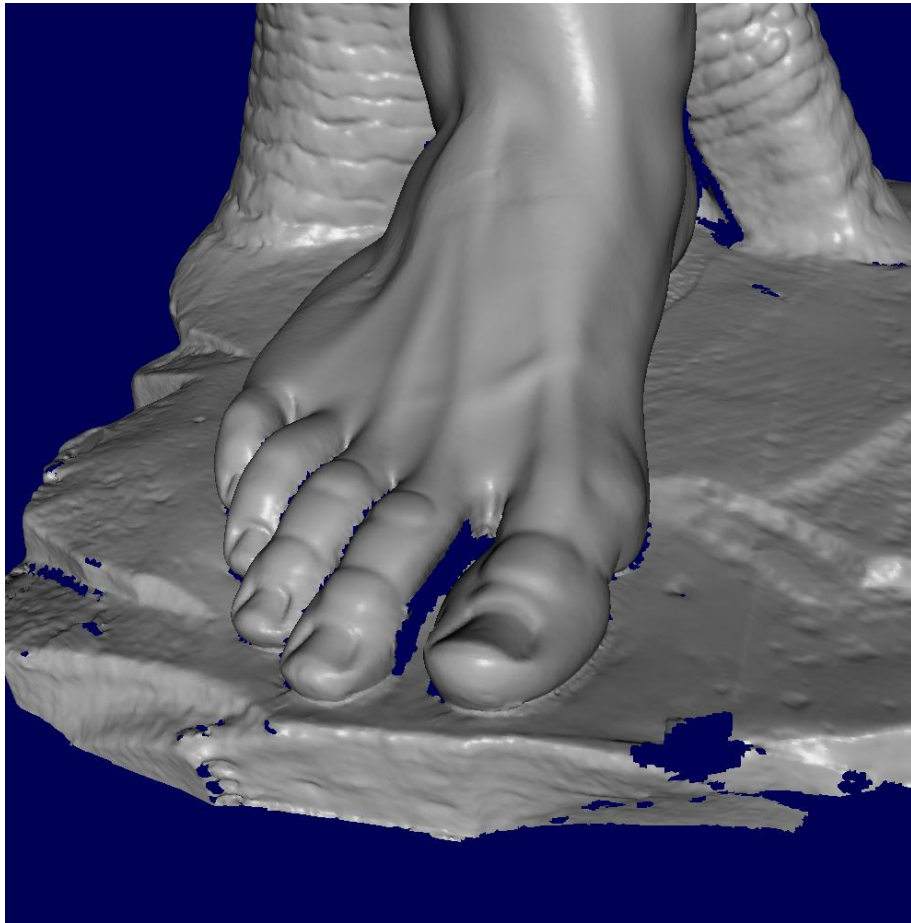
Surface Inpainting

[Davis et al., 3DPVT 2002]

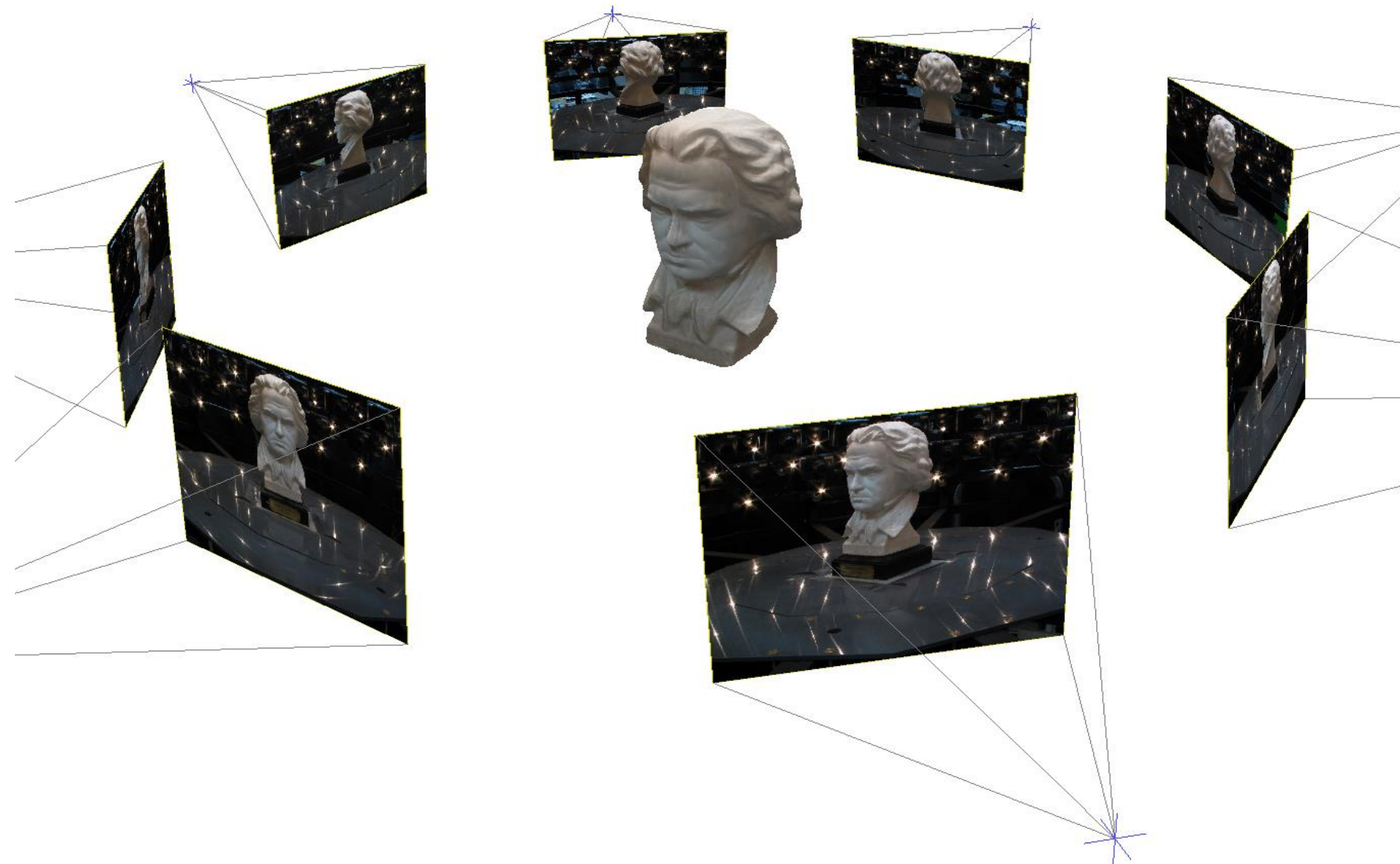


Surface Inpainting

[Davis et al., 3DPVT 2002]



Multi-View 3D Reconstruction



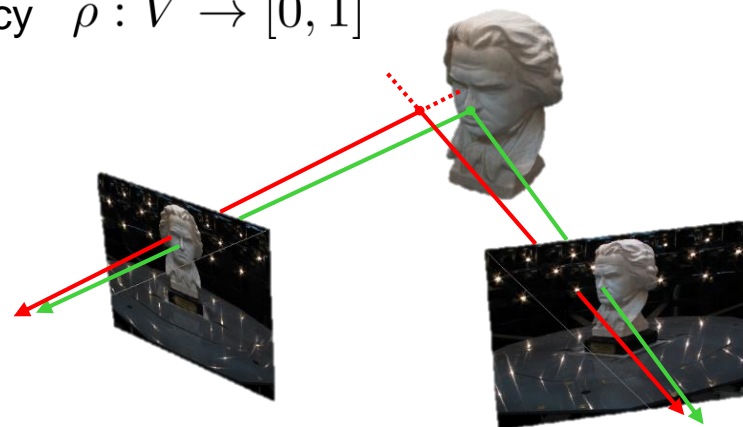
Multi-View 3D Reconstruction

Interior/exterior labeling $u : V \rightarrow \{0, 1\}$

$$\min_u \int_V \rho |\nabla u| dx + \lambda \int_V f u dx$$

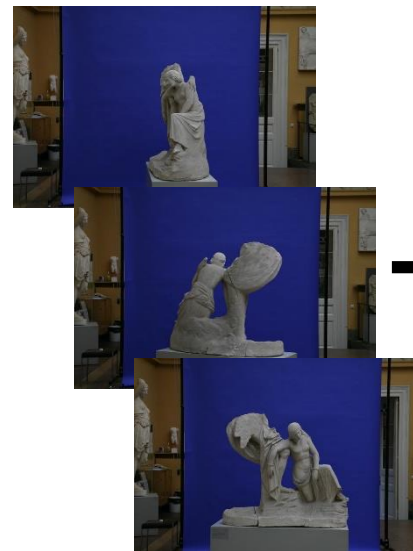
weighted TV + data term

Photo-consistency $\rho : V \rightarrow [0, 1]$



[Kolev et al., IJCV 2009]

Reconstructing the Niobids statues (450 B.C.)

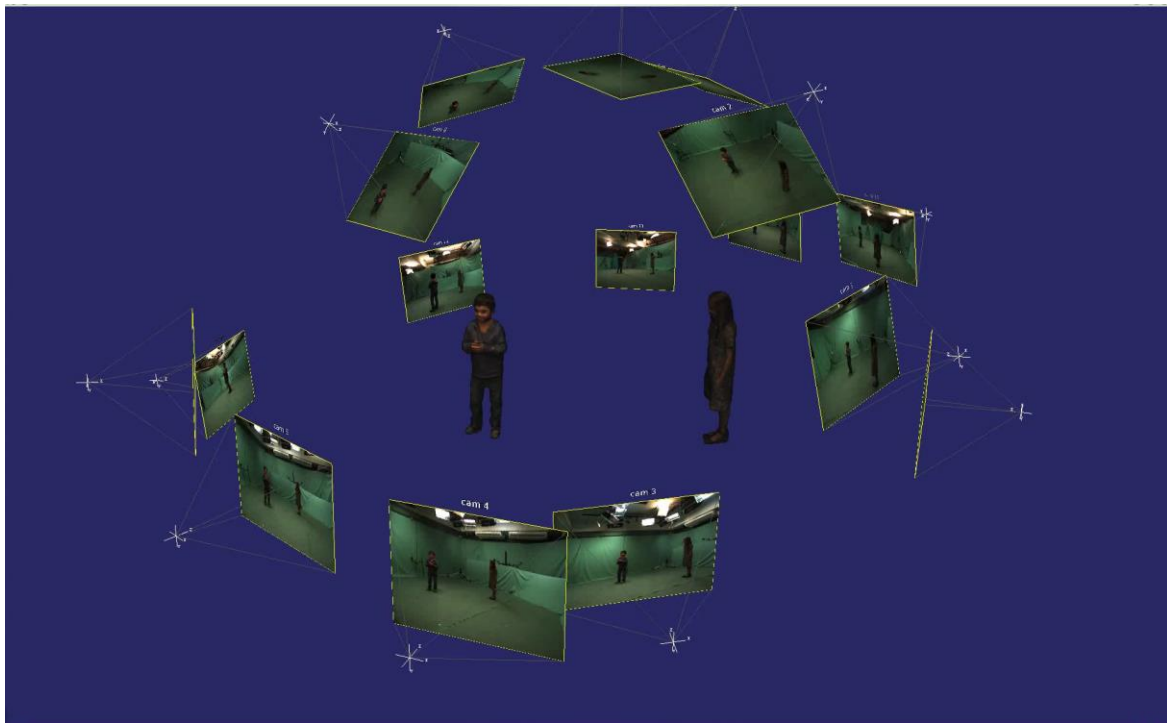
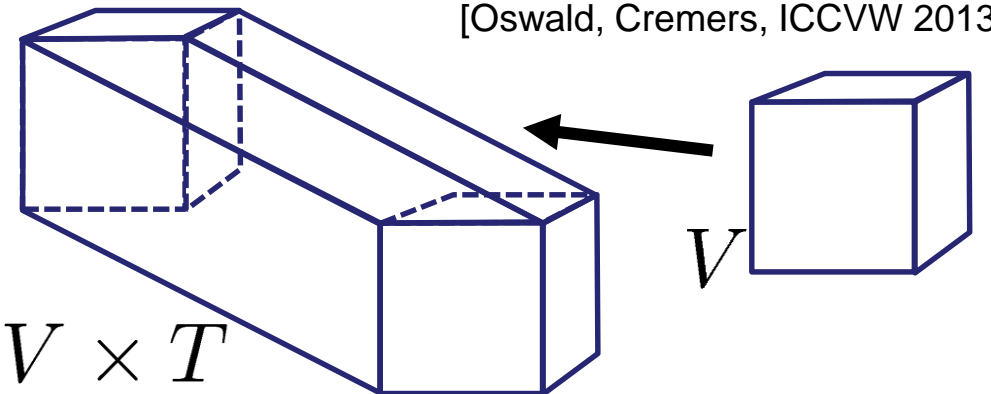


Space-time 3D Reconstruction

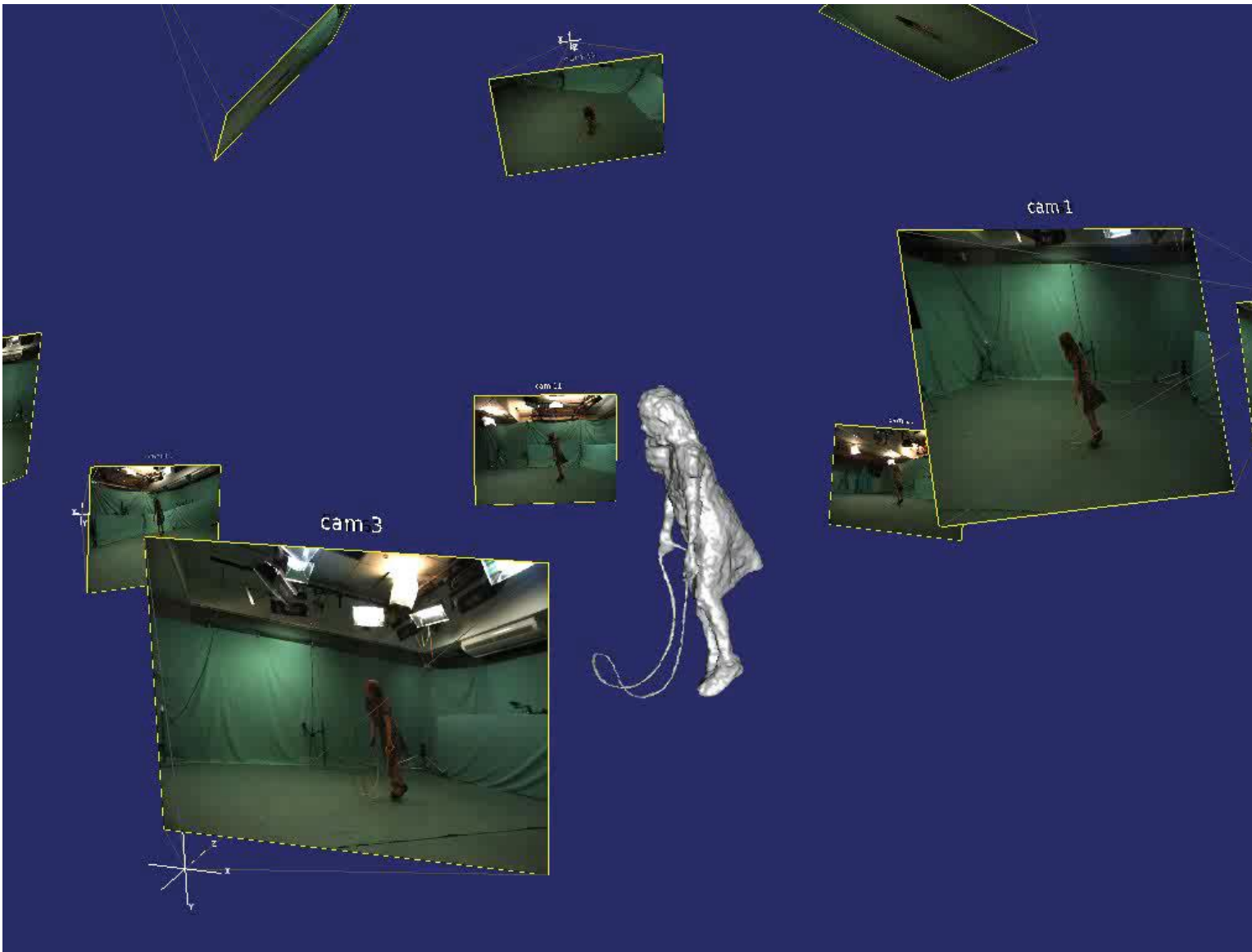
Interior/exterior labeling $u : V \times T \mapsto \{0, 1\}$

$$\min_u \int_{V \times T} (\rho |\nabla_x u| + g_t |\nabla_t u|) dx dt + \lambda \int_{V \times T} f u dx dt$$

spatial regularization term temporal regularization term data term



Space-time 3D Reconstruction



[Oswald, Cremers, ECCV 2014]

Single-View Reconstruction

input: image $I : \Omega \mapsto \mathbb{R}^3$
silhouette information $S \subset \Omega$

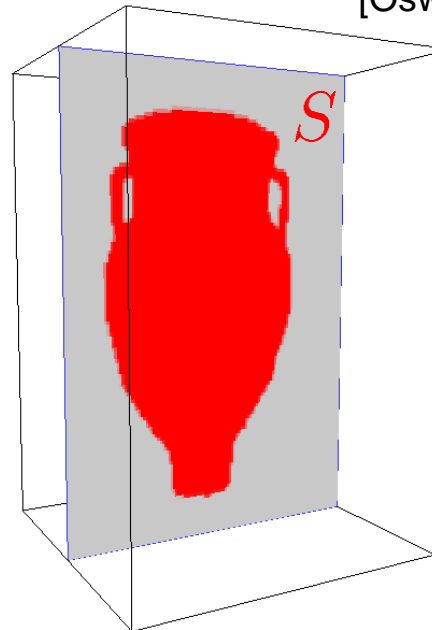
output: closed surface $\Sigma \subset \mathbb{R}^3$

implicit representation:

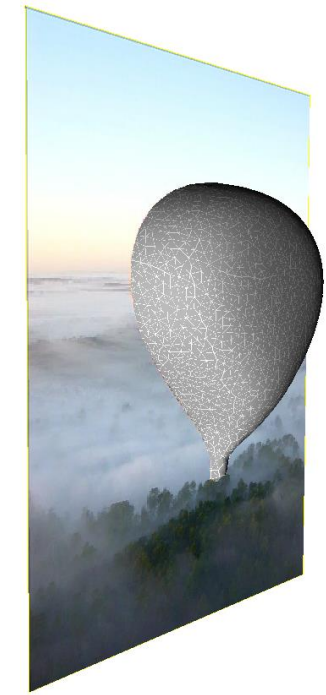
$$u : V \rightarrow \{0, 1\}, u(x) := \begin{cases} 1 & \text{if } x \in \text{int}(\Sigma) \\ 0 & \text{otherwise} \end{cases}$$

$$u^* = \arg \min_{u \in U_S \cap U_V} \int_V |\nabla u| dx$$

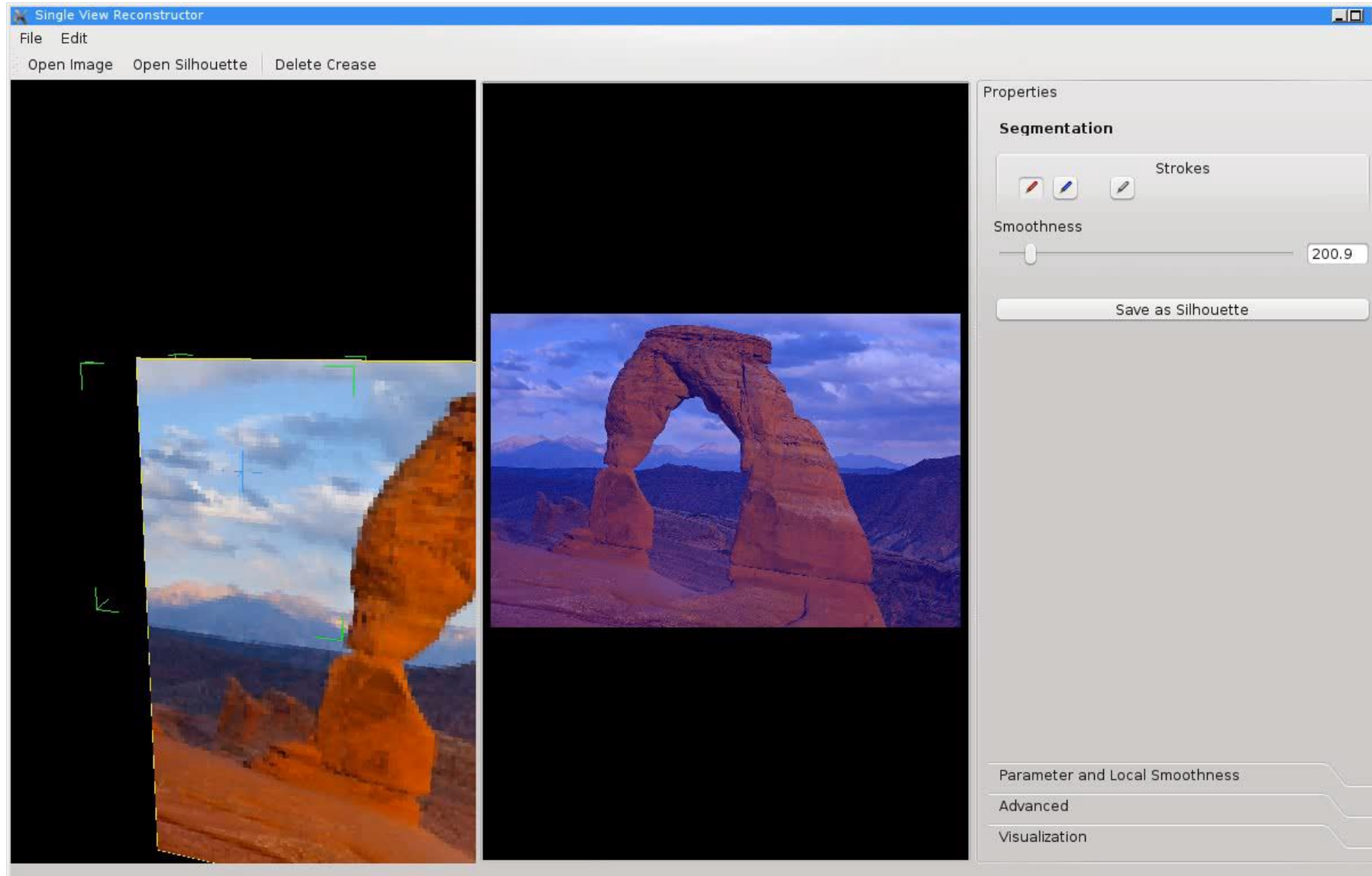
$$U_V = \left\{ u \mid \int_V u(x) dx = V_t \right\}$$



[Oswald, Töppe, Cremers, Rother, ACCV 2010]



Single-View Reconstruction



[Oswald, Töppe,
Cremers, Rother, ACCV 2010]

Generalization of Regularizers

The thresholding theorem (i.e. equivalence of minimizers for relaxed and binary problems) have been shown for the following regularizers:

Isotropic (all normal directions are equally penalized)

- spatially homogeneous TV

[Chan et al, 2006] (unit circle shape)

-> smooth all directions equally,
everywhere in the image

$$\phi_{\mathbf{x}}(v) = \|v\|_2$$

- spatially varying weighted TV

[Bresson et al., 2007] (scaled circle shape)

-> down-weight certain locations in the image
independent of the direction (reduces smoothness cost to allow for local transitions)

$$\phi_{\mathbf{x}}(v) = g(x) \|v\|_2$$

Anisotropic (some normal directions are penalized more than others)

- anisotropic spatially varying TV

[Olsson et al., 2009] (ellipsoidal shape)

-> down-weight certain directions
wrt. a given normal direction (smoothes along, but not across edges)

$$\phi_{\mathbf{x}}(v) = \sqrt{v(x)^T D_x v(x)}$$

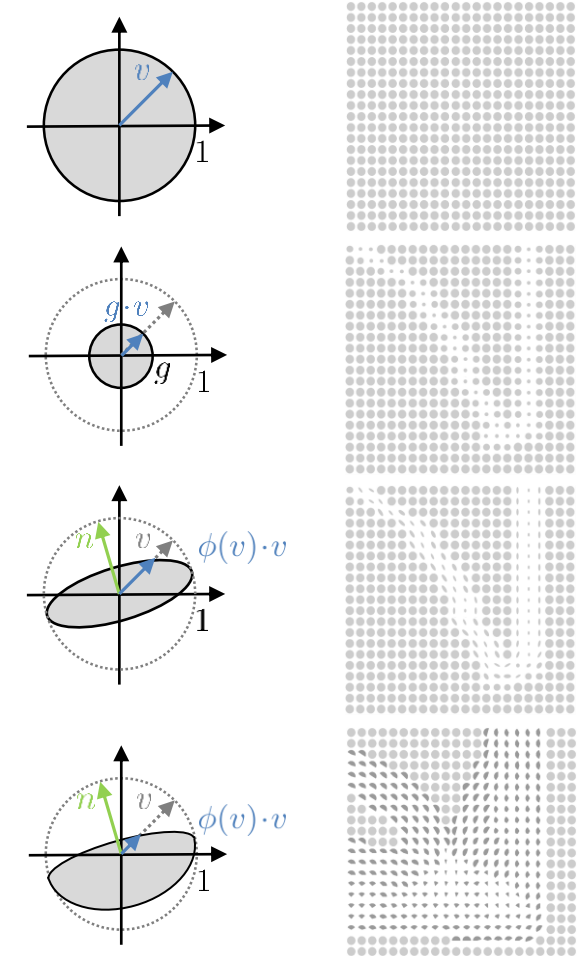
- anisotropic spatially varying Wulff shape

[Zach et al., 2009] (general convex shape)

-> down-weight certain directions
wrt. some given alignment (prefers certain gradient directions for local transitions)

$$\phi_{\mathbf{x}}(v) = \max_{\mu \in W_\phi} \langle \mu, v \rangle$$

$$E(u) = \int_{\Omega} (\phi_{\mathbf{x}}(\nabla u) + \lambda f u) \, d\mathbf{x}$$



Anisotropic Regularization

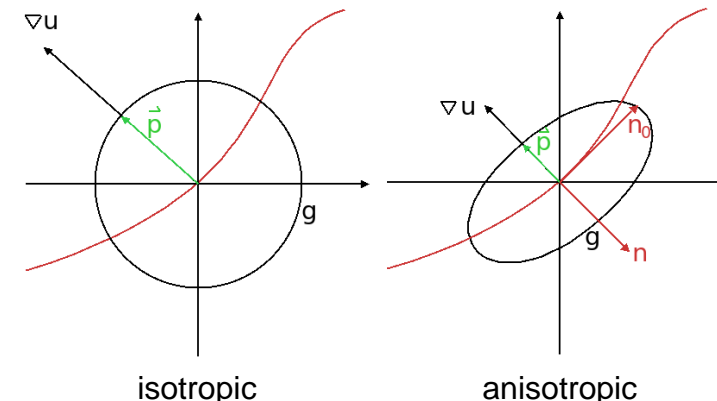
Idea: smooth along edges, but not across edges
-> better preserves fine-scaled structures

$$\phi_{\mathbf{x}}(v) = \sqrt{v(x)^T D_x v(x)}$$

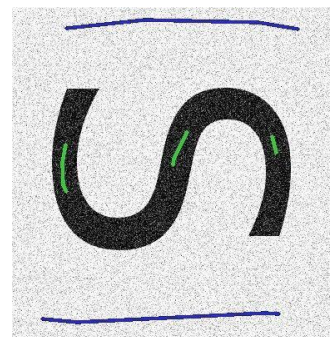
$$D_x = g(x)^2 nn^T + n_0 n_0^T + n_1 n_1^T$$

$$n(x) = \frac{\nabla I(x)}{\|\nabla I(x)\|_2} \quad n \perp n_0 \quad n_1 = n \times n_0$$

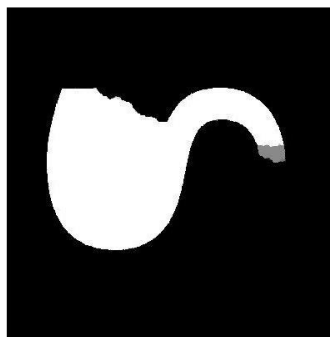
$$g(x) = \exp(-\beta |\nabla I(x)|^\alpha)$$



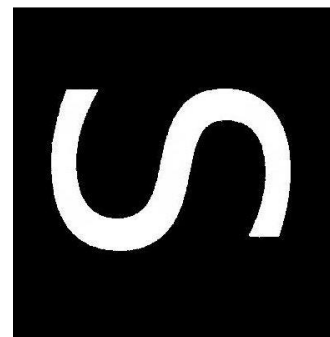
input image



input with noise and scribbles



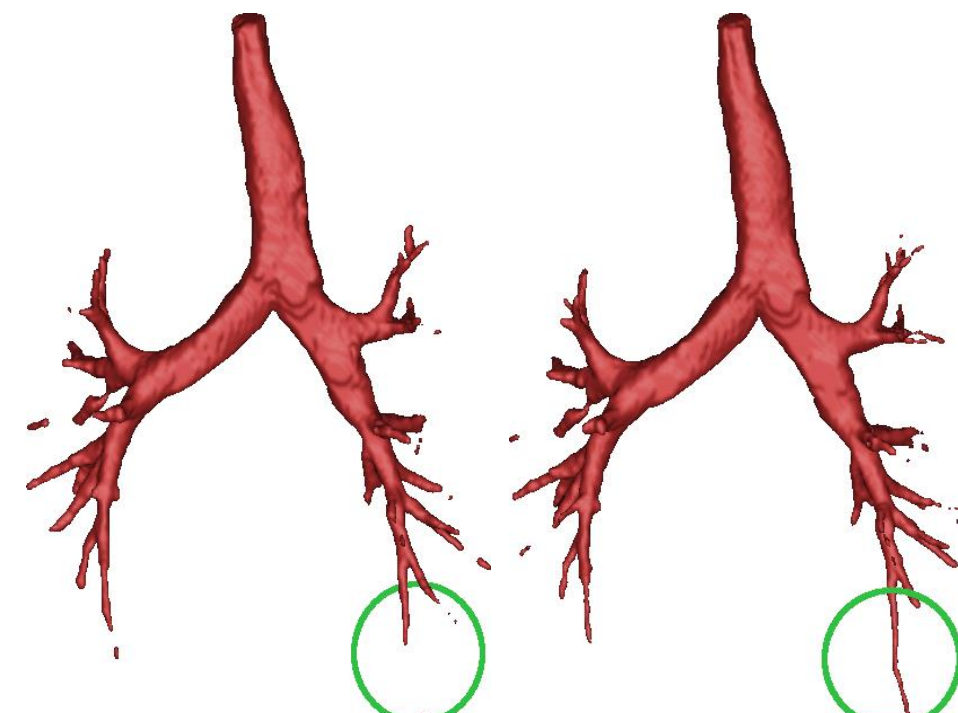
segmentation with isotropic regularization



Segmentation with anisotropic regularization

$$E(u) = \int_{\Omega} (\phi_{\mathbf{x}}(\nabla u) + \lambda f u) dx$$

[Reinbacher et al., ECCV 2010]



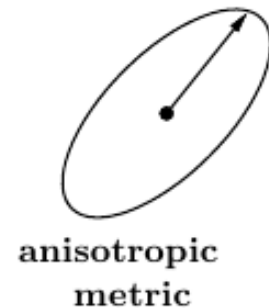
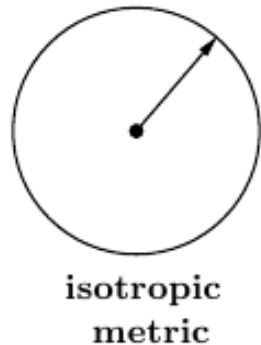
Anisotropic Regularization

Idea: use estimated surface normals to better preserve surface details

[Kolev et al., ECCV 2008]

$$\phi_{\mathbf{x}}(v) = \sqrt{v(x)^T D_x v(x)}$$

$$E(u) = \int_{\Omega} (\phi_{\mathbf{x}}(\nabla u) + \lambda f u) dx$$



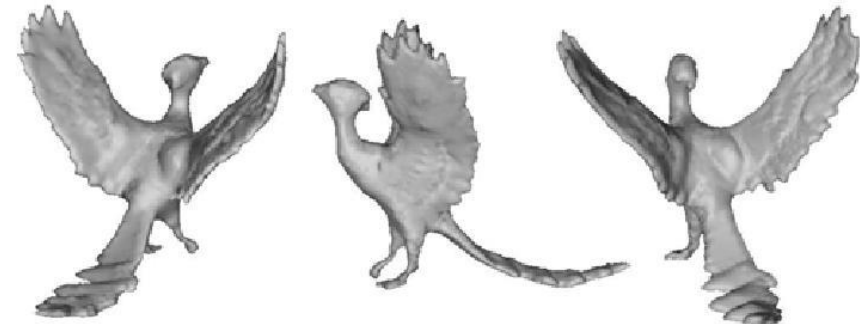
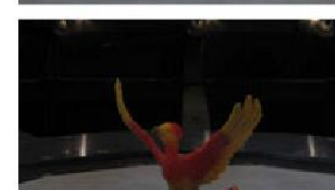
input image



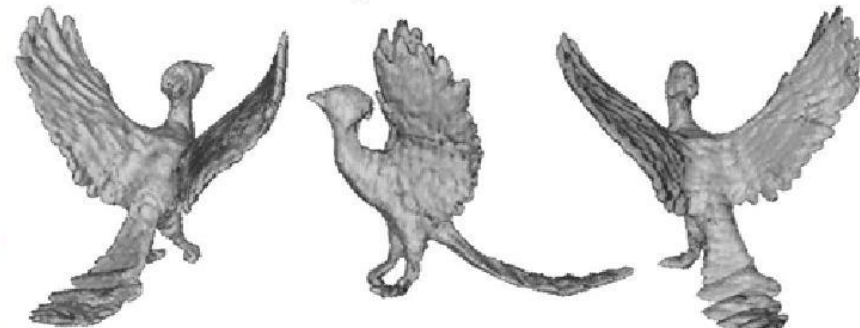
point cloud



surface normals



isotropic minimal surface



anisotropic minimal surface

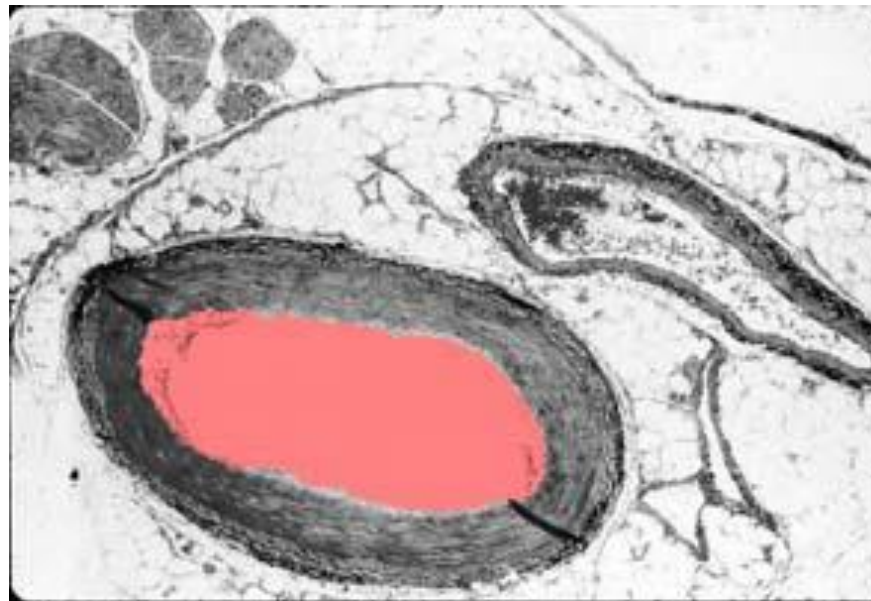
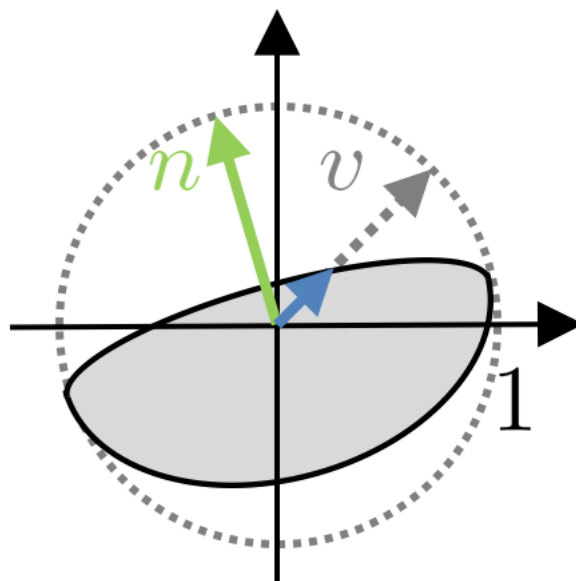
General Anisotropic Regularization

Idea: use estimated image gradients to prefer corresponding normal directions and normal orientations.

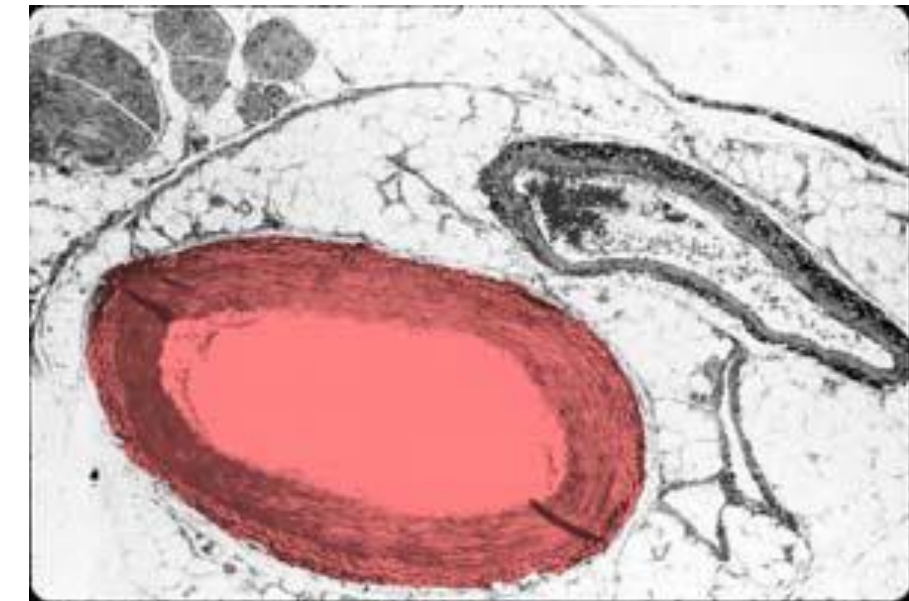
[Zach et al., DAGM 2009]

$$\phi_{\mathbf{x}}(v) = \max_{\mu \in W_\phi} \langle \mu, v \rangle$$

$$E(u) = \int_{\Omega} (\phi_{\mathbf{x}}(\nabla u) + \lambda f u) \, d\mathbf{x}$$



weighted isotropic regularization
(snaps to next gradient)

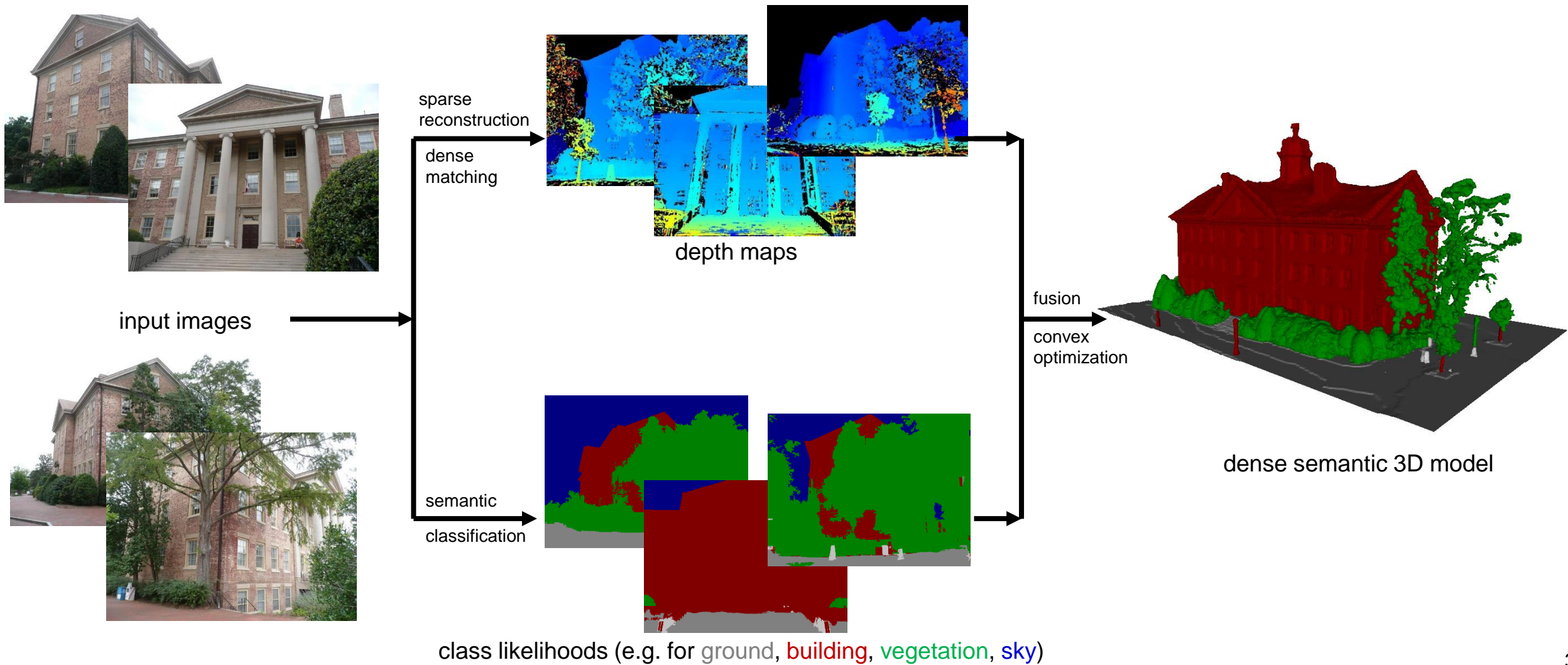


anisotropic Wulff-shape regularization
(snaps to next dark->bright gradient)

Joint Semantic Classification and 3D Reconstruction

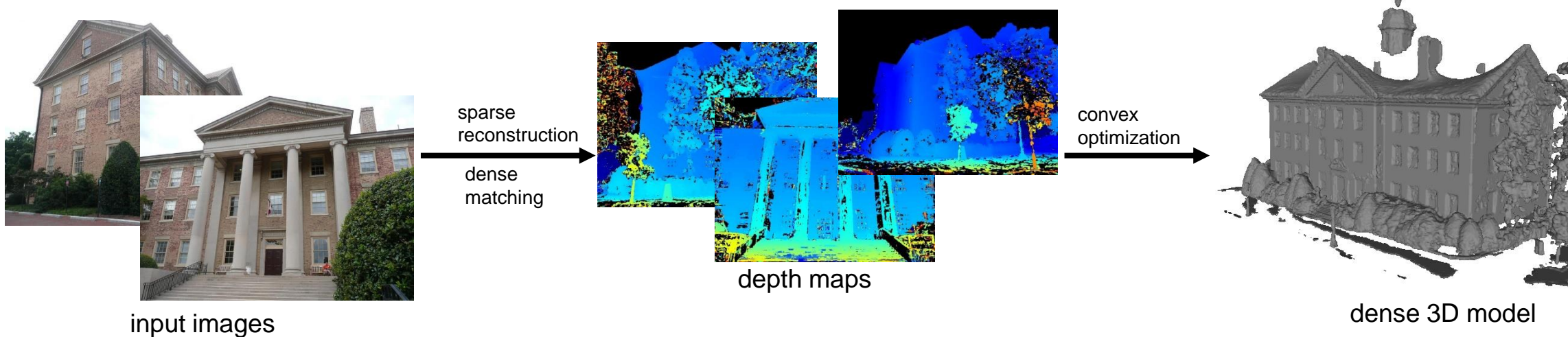
Pipeline overview

[Häne et al., CVPR 2013]



Joint Semantic Classification and 3D Reconstruction

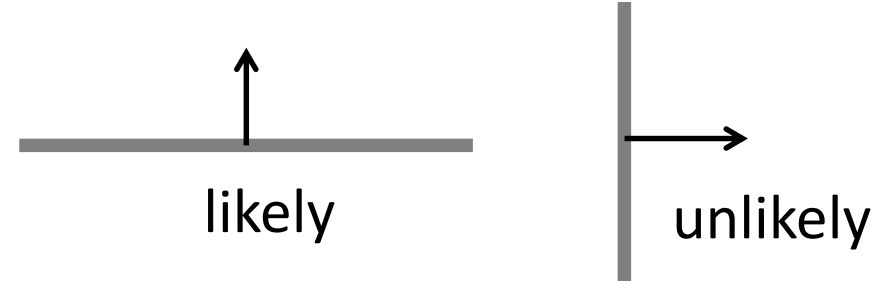
Previous Pipeline



[Häne et al., CVPR 2013]

Many parts like the ground are not properly reconstructed.

Observation: Likelihoods for “ground” surface normals

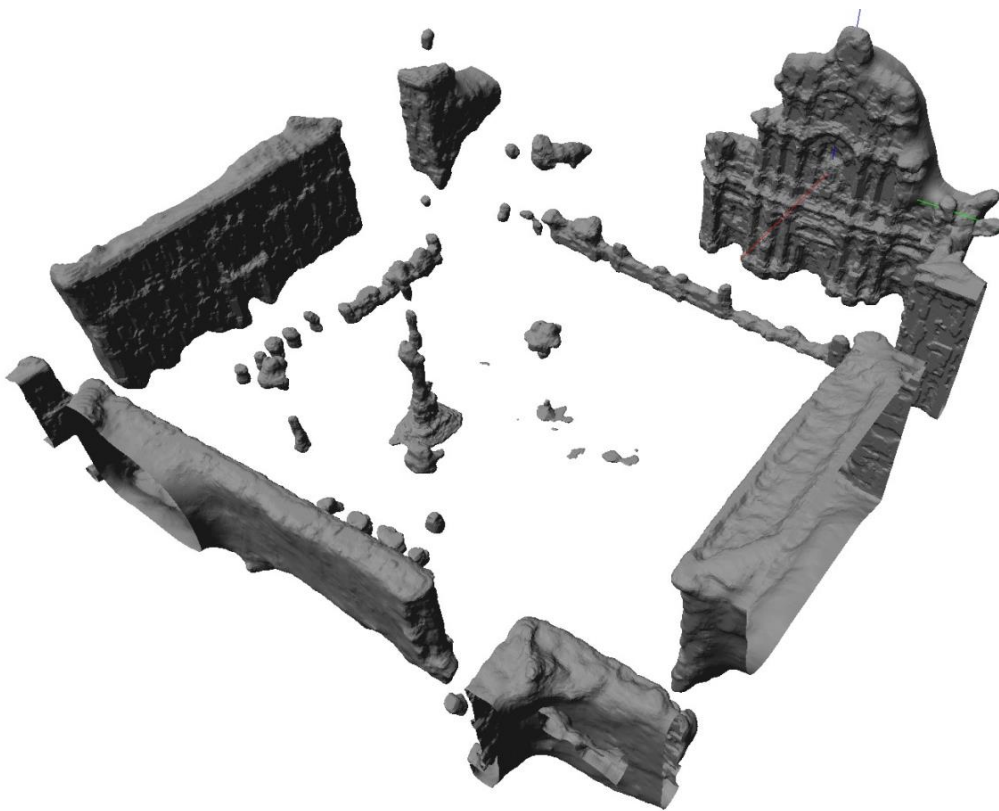


Idea: Learn common normal distributions for each class and corresponding class interaction likelihoods from data and use this information as a prior during joint reconstruction and classification.

Joint Semantic Classification and 3D Reconstruction

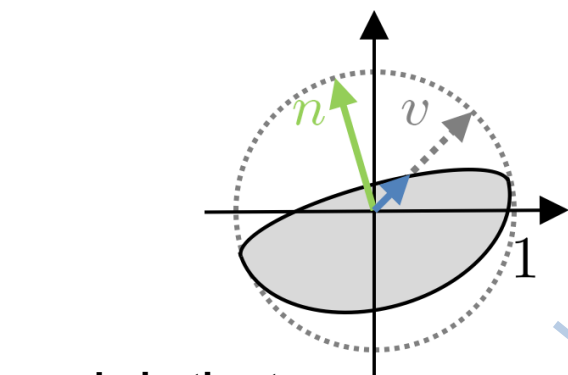


[Häne et al., CVPR 2013]



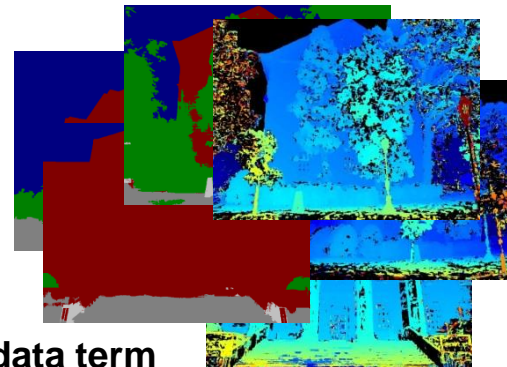
Joint Semantic Classification and 3D Reconstruction

[Häne et al., CVPR 2013]



regularization term

Class-specific, direction dependent,
surface area penalization



data term

Class-specific, direction dependent,
surface area penalization

$$E(x, y) = \sum_{s \in \Omega} \left(\sum_{i,j:i < j} \phi^{ij}(y^{ij}) + \sum_i \rho_s^i x_s^i u \right)$$

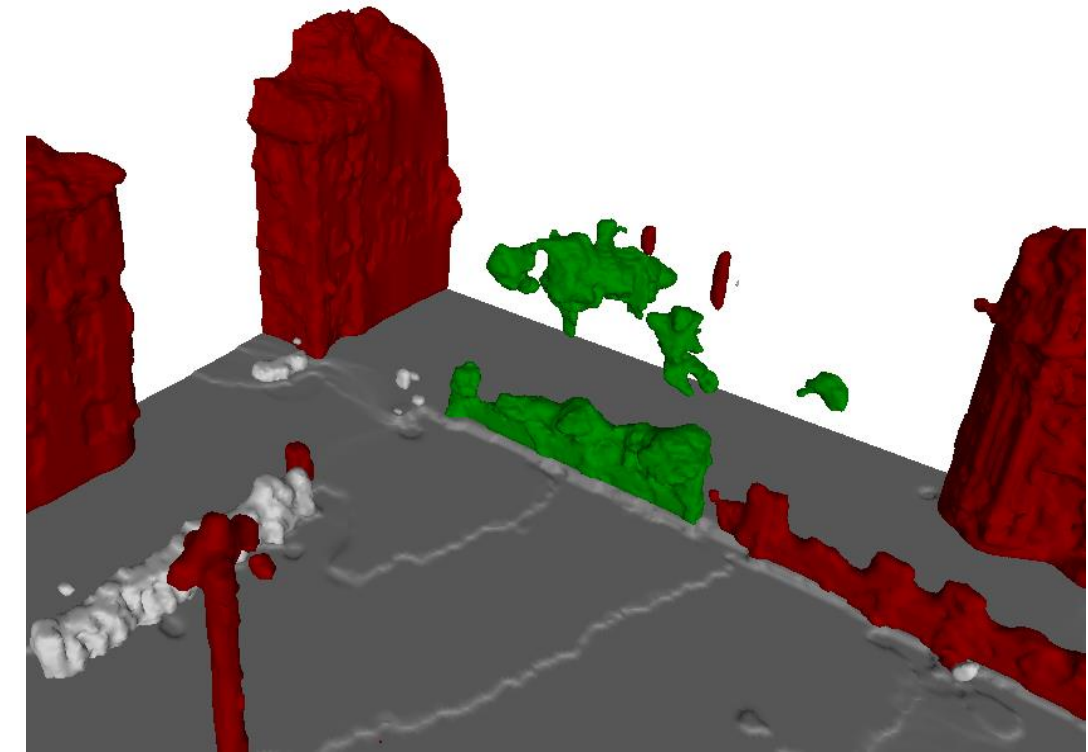
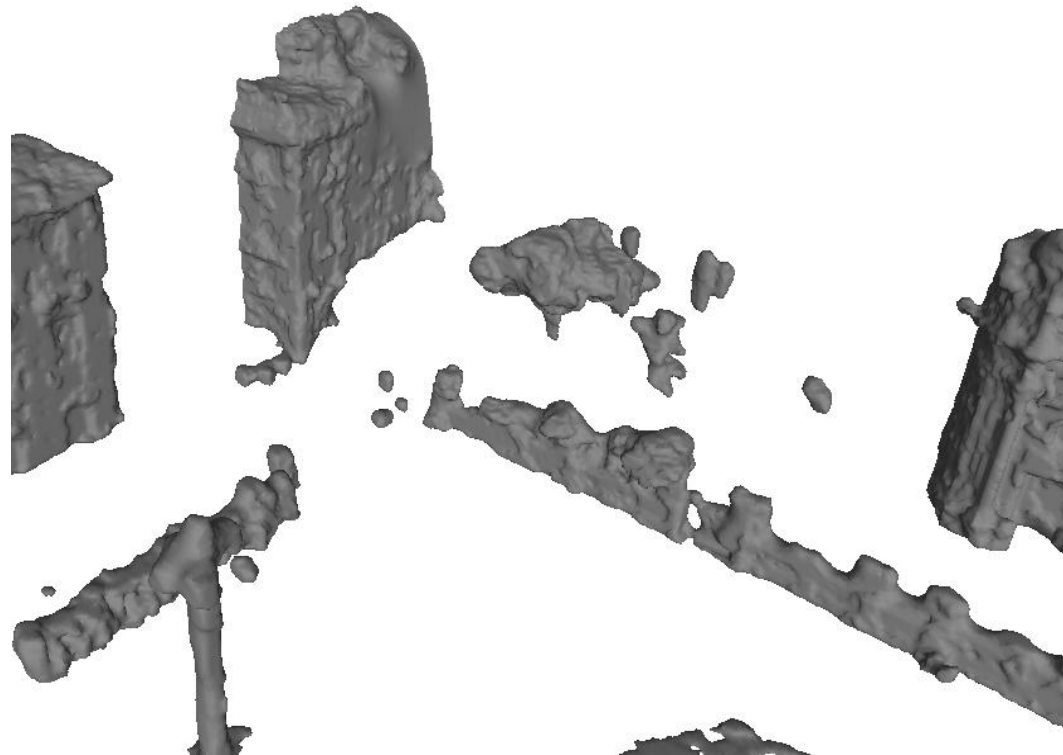
learned from
training data



Joint Semantic Classification and 3D Reconstruction

[Häne et al., CVPR 2013]

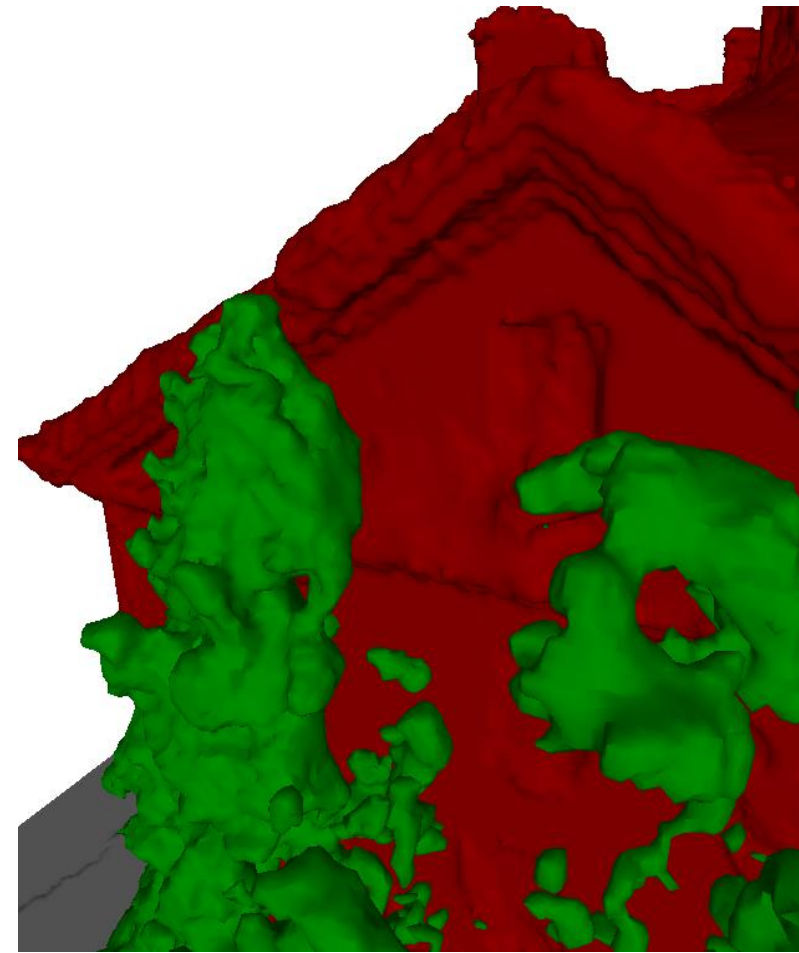
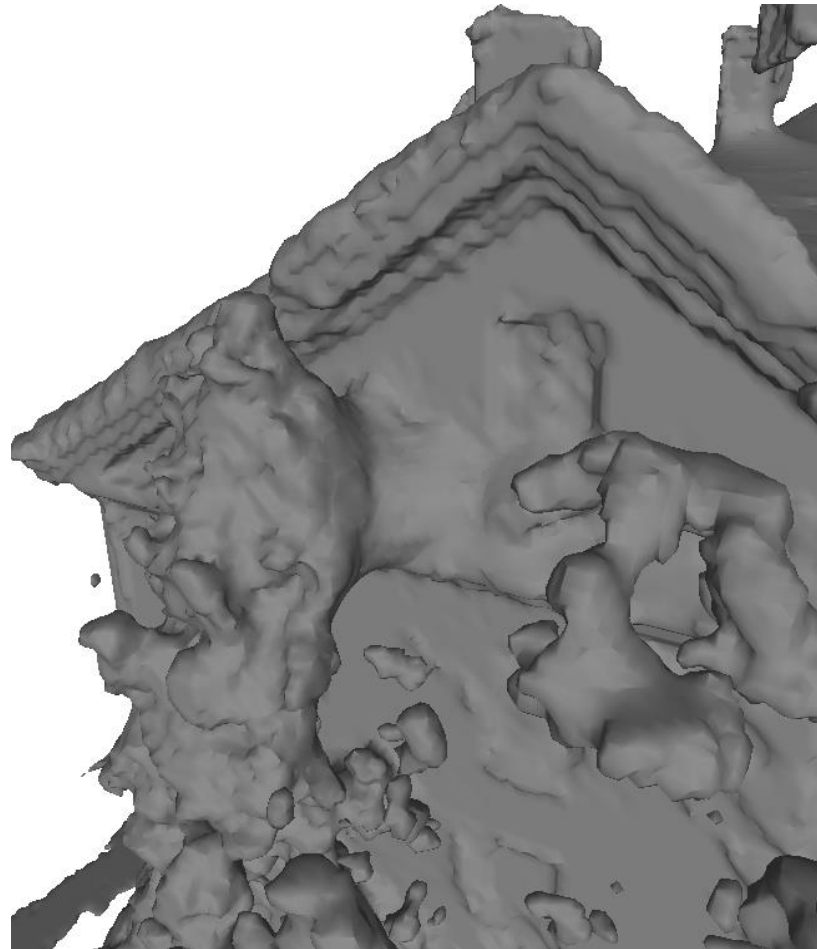
Weakly observed structures are completed by the prior:
The ground is mostly flat, buildings stand on the ground.



Joint Semantic Classification and 3D Reconstruction

Buildings are separated from vegetation.

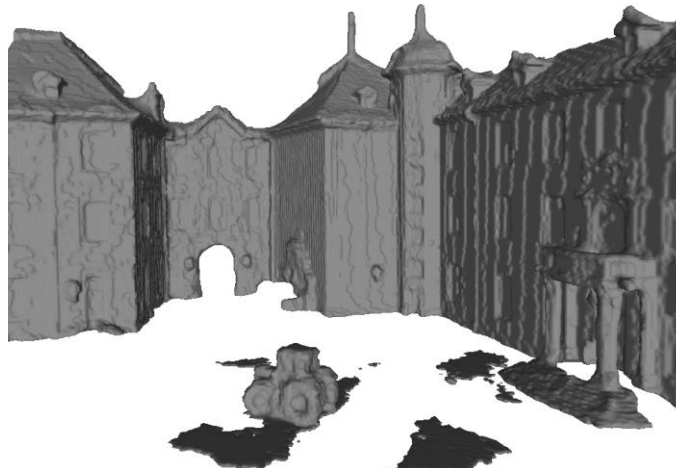
[Häne et al., CVPR 2013]



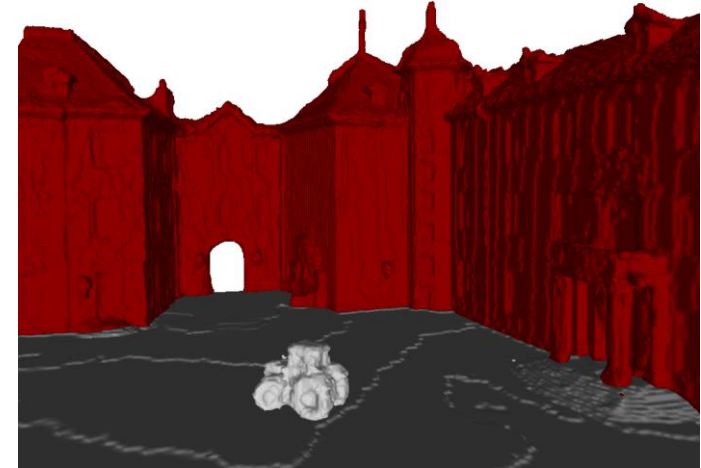
Joint Semantic Classification and 3D Reconstruction



input image

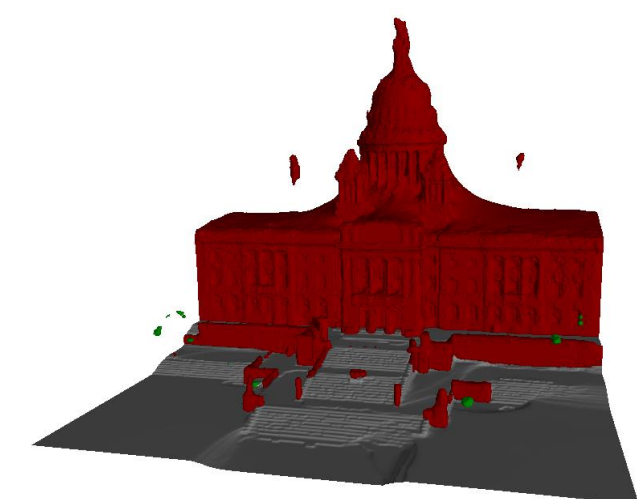
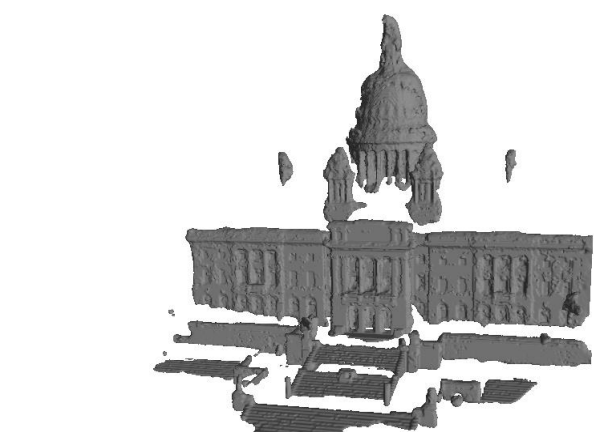


dense 3D reconstruction



semantic 3D reconstruction

[Häne et al., CVPR 2013]



References

- W. H. Meeks III and J. Pérez. “*A Survey on Classical Minimal Surface Theory*”. University lecture series. American Mathematical Society, 2012
- J. Davis S.R., Marschner, M. Garr, M. Levoy, “*Filling Holes in Complex Surfaces using Volumetric Diffusion.*”, International Symposium on 3D Data Processing, Visualization, Transmission (3DPVT), 2002
- K. Kolev, T. Pock, D. Cremers. “*Anisotropic minimal surfaces integrating photoconsistency and normal information for multiview stereo*”, ECCV, 2010
- C. Reinbacher, T. Pock, C. Bauer, H. Bischof, “*Variational segmentation of elongated volumetric structures*”, CVPR, 2010
- K. Kolev, M. Klodt, T. Brox, D. Cremers. “*Continuous global optimization in multiview 3d reconstruction*”, IJCV, 84(1):80–96, 2009
- Martin R. Oswald, Daniel Cremers, “*A convex relaxation approach to space time multi-view 3D reconstruction*”, ICCVW (4DMOD), 2013
- Martin R. Oswald, Jan Stühmer, and Daniel Cremers, “*Generalized connectivity constraints for spatio-temporal 3D reconstruction*”, ECCV, 2014
- M. R. Oswald, E. Töppe, D. Cremers, C. Rother, “*Image-based 3D modeling via cheeger sets*”, ACCV, 2010
- T. Pock, D. Cremers, H. Bischof, and A. Chambolle, “*An algorithm for minimizing the piecewise smooth Mumford-Shah functional.*”, In ECCV, 2008.
- M. Klodt, T. Schoenemann, K. Kolev, M. Schikora, D. Cremers, “*An Experimental Comparison of Discrete and Continuous Shape Optimization Methods*”, European Conference on Computer Vision (ECCV), 2008
- T. Chan, S. Esedoglu, and M. Nikolova, “*Algorithms for finding global minimizers of image segmentation and denoising models.*”, SIAM Journal on Applied Mathematics, 66(5):1632–1648, 2006
- Xavier Bresson, Selim Esedoglu, Pierre Vandergheynst, Jean-Philippe Thiran, and Stanley Osher, “*Fast global minimization of the active contour/snake model.*”, Journal of Mathematical Imaging and Vision, 28(2):151–167, 2007
- C. Olsson, M. Byr öd, N. C. Overgaard, F. Kahl, “*Extending continuous cuts: Anisotropic metrics and expansion moves*”, ICCV, 2009
- Christopher Zach, Liang Shan, and Marc Niethammer, “*Globally Optimal Finsler Active Contours*”, DAGM-Symposium, volume 5748 of Lecture Notes in Computer Science, page 552-561. Springer, 2009
- C. Häne, C. Zach, A. Cohen, R. Angst, M. Pollefeys, “*Joint 3d scene reconstruction and class segmentation*”, CVPR, 2013